

AFFDL-TR-76-14
Volume I

12

FL

ADA033594

**STABILITY OF FLAT, SIMPLY SUPPORTED,
RECTANGULAR SANDWICH PANELS
SUBJECTED TO COMBINED INPLANE
LOADINGS
THEORETICAL DEVELOPMENT**

*UNIVERSITY OF DAYTON
RESEARCH INSTITUTE
DAYTON, OHIO*

SEPTEMBER 1976

TECHNICAL REPORT AFFDL-TR-76-14 Volume I
FINAL REPORT FOR PERIOD NOVEMBER 1974 - JUNE 1975

Approved for public release; distribution unlimited

DDC
RECEIVED
DEC 20 1976
A

AIR FORCE FLIGHT DYNAMICS LABORATORY
AIR FORCE WRIGHT AERONAUTICAL LABORATORY
AIR FORCE SYSTEMS COMMAND
WRIGHT-PATTERSON AIR FORCE BASE, OHIO 45433

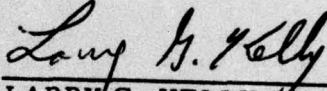
NOTICE

When Government drawings, specifications, or other data are used for any purpose other than in connection with a definitely related Government procurement operation, the United States Government thereby incurs no responsibility nor any obligation whatsoever; and the fact that the government may have formulated, furnished, or in any way supplied the said drawings, specifications, or other data, is not to be regarded by implication or otherwise as in any manner licensing the holder or any other person or corporation, or conveying any rights or permission to manufacture, use, or sell any patented invention that may in any way be related thereto.

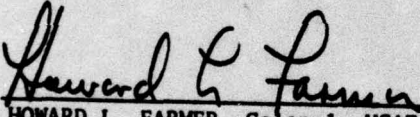
This technical report has been reviewed and is approved for publication.

This report has been reviewed by the Information Office (OI) and is releasable to the National Technical Information Service (NTIS). At NTIS, it will be available to the general public, including foreign nations.


HAROLD C. CROOP,
Project Engineer


LARRY G. KELLY, Chief
Structural Development Branch
Structural Mechanics Division

FOR THE COMMANDER


HOWARD L. FARMER, Colonel, USAF
Chief, Structural Mechanics Division

Copies of this report should not be returned unless return is required by security considerations, contractual obligations, or notice on a specific document.

UNCLASSIFIED

SECURITY CLASSIFICATION OF THIS PAGE (When Data Entered)

19 REPORT DOCUMENTATION PAGE		READ INSTRUCTIONS BEFORE COMPLETING FORM
1. REPORT NUMBER AFFDL-TR-76-14-VOLUME 1-1	2. GOVT ACCESSION NO.	3. RECIPIENT'S CATALOG NUMBER
4. TITLE (and Subtitle) STABILITY OF FLAT, SIMPLY SUPPORTED, RECTANGULAR SANDWICH PANELS SUBJECTED TO COMBINED INPLANE LOADINGS.	5. TYPE OF REPORT & PERIOD COVERED Final Report 11/74 - 6/75	6. PERFORMING ORG. REPORT NUMBER UDRI-TR-75-51
7. AUTHOR(s) R.A. Brockman	8. CONTRACT OR GRANT NUMBER(s) F33615-75-C-3009 NEW	9. PROGRAM ELEMENT, PROJECT, TASK AREA & WORK UNIT NUMBERS 13680217 62201 F 1202
9. PERFORMING ORGANIZATION NAME AND ADDRESS University of Dayton Research Institute 300 College Park Avenue Dayton, Ohio 45469	10. CONTROLLING OFFICE NAME AND ADDRESS Air Force Flight Dynamics Laboratory, FBS Wright-Patterson AFB, Ohio 45433	11. REPORT DATE Sep 76
11. MONITORING AGENCY NAME & ADDRESS (if different from Controlling Office)	12. NUMBER OF PAGES 46	13. SECURITY CLASS. (of this report) Unclassified
12. DISTRIBUTION STATEMENT (of this Report) Final rept. Nov 74 - Jun 75	14. DISTRIBUTION STATEMENT (of the abstract entered in Block 20, if different from Report)	15a. DECLASSIFICATION/DOWNGRADING SCHEDULE 1257p.
Approved for public release; distribution unlimited.		
14 UDRI-TR-75-51-Vol-1		
18. SUPPLEMENTARY NOTES		
19. KEY WORDS (Continue on reverse side if necessary and identify by block number)		
structural analysis	flat plate	Ritz Method
structural sandwich composites	buckling	combined load
layered structure	elastic stability	flat panel
sandwich panel	potential energy	simply supported
20. ABSTRACT (Continue on reverse side if necessary and identify by block number)		
The general stability of flat, rectangular sandwich panels loaded by combined biaxial compression, biaxial edgewise bending and edgewise shear is investigated. The analysis is applicable to sandwich structures having isotropic face sheets and orthotropic cores. The analysis procedure is based upon a linear potential energy formulation and the Ritz method of discretization. For the case of simply supported boundaries, it is shown that the equations		

105400-
LB

UNCLASSIFIED

SECURITY CLASSIFICATION OF THIS PAGE(When Data Entered)

19. Keywords (Continued)

edgewise compression
edgewise bending
edgewise shear
inplane loads
interaction formula

20. Abstract (Continued)

can be uncoupled in such a way that a numerical solution is obtained in an economical fashion. A number of verification results are presented. Comparisons are made between the numerical solutions and the predictions of certain interaction formulas which are commonly employed in sandwich panel design.

UNCLASSIFIED

SECURITY CLASSIFICATION OF THIS PAGE(When Data Entered)

FOREWORD

The work reported herein was performed by the Aerospace Mechanics Division of the University of Dayton Research Institute, Dayton, Ohio, under Air Force Contract F33615-75-C-3009, for the Air Force Flight Dynamics Laboratory, Wright-Patterson Air Force Base, Ohio. This effort was directed under Task 02 of Project 1368, "Structural Sandwich Composites". Technical direction and support was provided by Mr. Harold C. Croop (AFFDL/FBS) as Air Force Project Engineer.

The work described was conducted during the period between November 1974 and June 1975, under the general supervision of Mr. Dale H. Whitford Supervisor, Aerospace Mechanics Division, and Mr. George J. Roth, Leader, Structural Analysis Group. The principal investigator was Dr. Fred K. Bogner.

The author gratefully acknowledges the University of Dayton Research Library for providing reference materials on a timely basis, and the secretaries and Graphic Arts Section of the University for their help in the preparation of the report. Particular thanks are extended to Dr. Fred K. Bogner for his efforts in reviewing the material for technical accuracy and clarity, and to Mr. Harold C. Croop for numerous suggestions concerning its preparation.

ADDITIONAL	
RTIS	<input checked="" type="checkbox"/>
DOC	<input type="checkbox"/>
UNASSIGNED	<input type="checkbox"/>
JUSTIFIED	<input type="checkbox"/>
BY	
DISTRIBUTION - BY AIR MAIL	
Dist.	
A	

TABLE OF CONTENTS

SECTION		PAGE
1	INTRODUCTION	1
	1.1 PROBLEM DEFINITION AND SCOPE	1
	1.2 METHOD OF SOLUTION	3
2	THEORETICAL APPROACH	5
	2.1 GEOMETRY	5
	2.2 BASIC EQUATIONS	5
	2.3 POTENTIAL ENERGY	10
3	NUMERICAL SOLUTION FOR BUCKLING LOADS	13
	3.1 DISCRETIZATION OF THE POTENTIAL ENERGY BY THE RITZ METHOD	13
	3.2 APPLICATION OF THE PRINCIPLE OF MINIMUM POTENTIAL ENERGY	19
	3.3 ASSEMBLY OF EQUATIONS FOR SOLUTION	21
4	SUMMARY OF RESULTS	24
	4.1 VERIFICATION EXAMPLES	24
	4.2 TYPICAL RESULTS FOR COMBINED LOADINGS	26
	4.3 COMPARISON WITH INTERACTION FORMULAS	30
	4.3.1 Interaction Formula for Combined Edgewise Shear and Compression	31
	4.3.2 Interaction Formula for Combined Edgewise Bending and Compression	35
	4.3.3 Interaction Formula for Combined Edgewise Bending and Shear	35
	4.4 DISCUSSION	42
5	SUMMARY AND CONCLUSIONS	43
6	REFERENCES	45

LIST OF ILLUSTRATIONS

FIGURE		PAGE
1	Applied Inplane Loads	2
2	Panel Geometry	6
3	Geometry of Deformation in the x-z Plane	7
4	Effect of a Shear Load Upon Critical Compressive Stress in Biaxial Loading	27
5	Effect of an Edgewise Bending Load Upon Critical Compressive and Shear Stresses	28
6	Error in Interaction Formula for Axial Compression and Edgewise Shear	33
7	Calculated Interaction Curves for Axial Compression and Edgewise Shear	34
8	Error in Interaction Formula for Edgewise Bending and Compression	37
9	Calculated Interaction Curves for Edgewise Bending and Compression	38
10	Error in Interaction Formula for Edgewise Shear and Bending	40
11	Calculated Interaction Curves for Edgewise Shear and Bending	41

LIST OF TABLES

TABLE		PAGE
1	Verification Results for Individual Critical Loads	25
2	Physical Data for Combined-Loads Examples	29
3	Comparison with Interaction Formula for Combined Biaxial Compression and Edgewise Shear	32
4	Comparison with Interaction Formula for Combined Edgewise Bending and Axial Compression	36
5	Comparison with Interaction Formula for Combined Edgewise Bending and Shear	39

LIST OF SYMBOLS

a, b	panel dimensions
a_{ij}	elements of a coefficient matrix in the potential energy; defined for each mode
b_i	elements of a coefficient vector in the potential energy; defined for each mode
c	subscript denoting core quantities
d	total depth of the sandwich panel
e_x, e_y	neutral plane locations
$f = 1, 2$	subscript denoting face quantities
h_{mn}, k_{mn}	undetermined parameters in potential energy
$n_{x_0}, n_{x_b}, n_{x_y},$ n_{y_b}, n_{y_0}	relative magnitudes of the applied inplane loads
t_1, t_2	face sheet thicknesses
t_c	core thickness
u_n, v_n	in plane displacements due to stretching
u, v, w	displacement components
x, y, z	Cartesian coordinates
A	coefficient matrix in the potential energy expression
B	coefficient vector in the potential energy expression
C	constant defined for each mode
E_1, E_2	Young's moduli of face sheets
G_{cxz}, G_{cyz}	core shear moduli
G	final geometric stiffness matrix

LIST OF SYMBOLS (Continued)

K	final stiffness matrix
$\bar{N}_x, \bar{N}_{xy}, \bar{N}_y$	total applied loads
$\bar{N}_{xo}, \bar{N}_{yo}$	edgewise compression load components
$\bar{N}_{xb}, \bar{N}_{yb}$	edgewise bending load components
W	work done by external forces
W_{mn}	assumed-mode parameters
$X_i; i=1, 4$	ratios of assumed-mode parameters
,	indicates partial differentiation with respect to the parameter following
$\alpha_{fx}, \alpha_{fy}, \beta_f$	geometric parameters
γ_{xyf}	shear strains in face sheets
$\gamma_{cxz}, \gamma_{cyz}$	core shear strains
δ	variational operator
δ_{ij}	Kronecker delta
$\epsilon_{xf}, \epsilon_{yf}$	extensional strains in face sheets
$\lambda_f = 1 - \nu_f^2$	face sheet parameters
λ	eigenvalue
ν_f	Poisson's ratios of face sheets
π_P	potential energy functional
$\sigma_{xf}, \sigma_{yf}, \tau_{xyf}$	face sheet stresses
τ_{cxz}, τ_{cyz}	core shear stresses
ϕ, ψ	core rotations in xz and yz planes

LIST OF SYMBOLS (Concluded)

Δ_{ij}	defined delta function
ϕ_{mn}, ψ_{mn}	assumed-mode parameters

SECTION 1

INTRODUCTION

A primary consideration in the design of structural sandwich components is the overall stability of a panel which is subjected to inplane loadings. These applied loads commonly consist of edgewise compression, edgewise shear and edgewise bending moments, as shown in Figure 1.

A large amount of literature is available concerning the buckling of flat, rectangular sandwich panels loaded by uniaxial edgewise compression^{1-6*}. Kuenzi, et al.⁷ have studied the problem of shear acting alone. Other investigators have considered the effects of compression combined with shear by the use of interaction formulas^{8,9} designed to account for interference between the various buckle patterns. The case of combined edgewise bending and compression has been investigated by Kimel¹⁰ with good results. The results of a similar study which considered combined bending, compression and shear¹¹ exhibited poor convergence behavior, particularly for cases in which the shear loads predominated.

This report presents a method for the prediction of the general instability of flat sandwich panels loaded by combined edgewise bending, biaxial compression and edgewise shear. It is anticipated that the method discussed herein will prove useful as a tool in both the design and the analysis of structural sandwich components.

1.1 PROBLEM DEFINITION AND SCOPE

The present analysis considers incipient buckling of flat, rectangular sandwich panels subjected to arbitrary combinations of biaxial edgewise

* Numerical superscripts indicate references listed in Section 6.

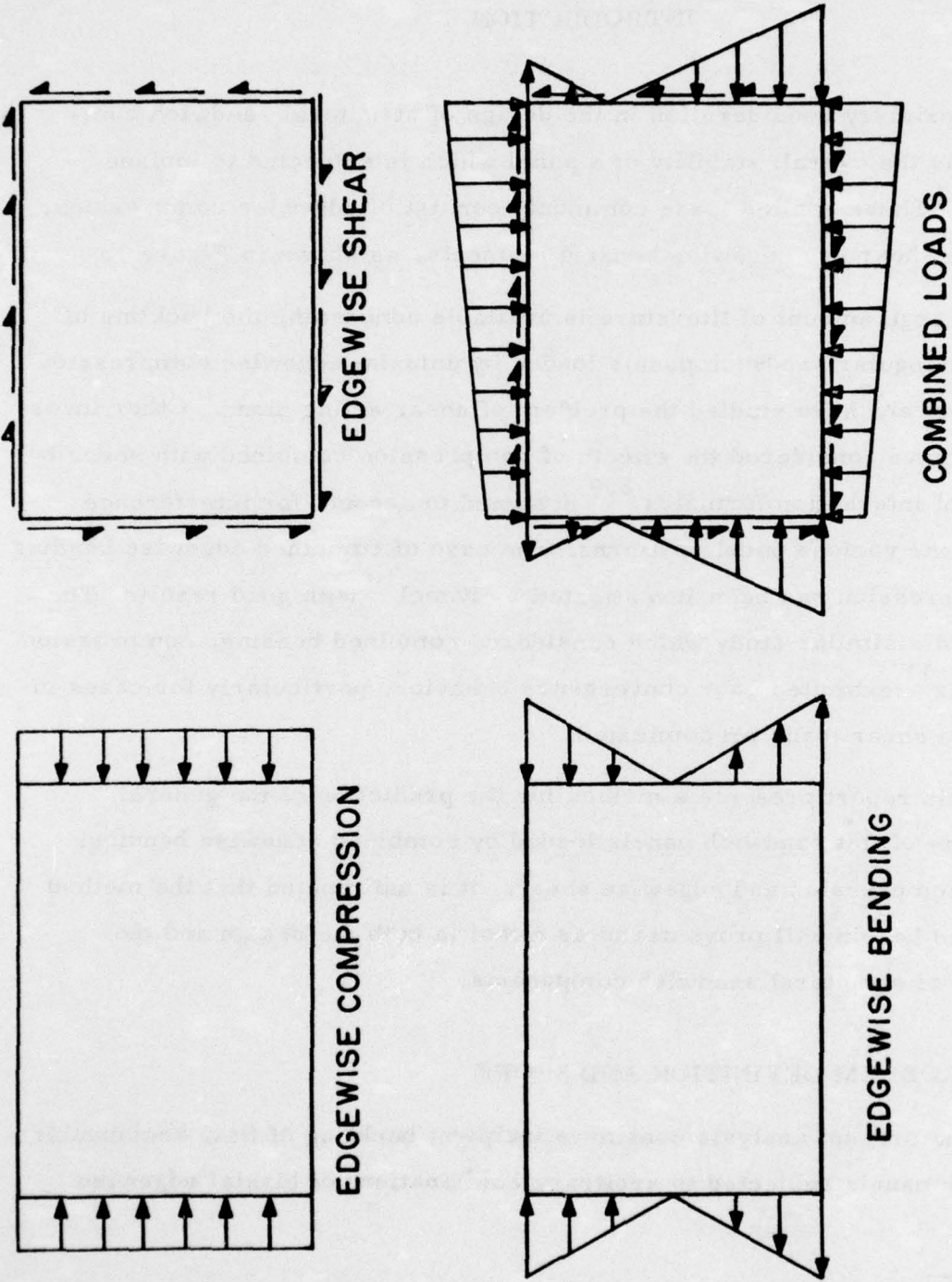


Figure 1. Applied Inplane Loads.

compression, edgewise bending and edgewise shear loadings. Only simply supported panels are considered, for which the component layers are restricted to linear elastic behavior and small displacements.

The core is considered to be completely rigid in the normal direction. The resistance of the core to extension and bending are assumed to be negligible; therefore the strain energy may be taken to consist only of contributions due to transverse shearing deformation. The transverse shear moduli of the core may be unequal, as is typical of many types of core construction.

Facing sheets are assumed to be isotropic and may have different properties and thicknesses.* Since the flexural rigidity of the faces is not neglected, critical combined loads of classical plates may be obtained as a special case (subject to the Love-Kirchhoff hypothesis).

1.2 METHOD OF SOLUTION

In general, linear analyses of sandwich deformations fall into two categories:¹² formulations in terms of face displacements, and analyses in terms of functions related to core displacements. The two methods are theoretically equivalent but permit slightly different numerical treatments of the boundary conditions.

The results presented herein are based upon the so-called "tilting method"¹³, by which the displacements in each layer of the sandwich are related to displacements in the core. A solution is obtained by using a discretization based on the Ritz method to minimize the total potential energy of the panel. As a means of uncoupling the flexural and extensional strain energies, it is postulated that a "neutral plane" exists in which no inplane displacements occur during the buckling deflection. The neutral

*The accurate analysis of severely unbalanced sandwich may require the use of a nonlinear technique. See Paragraph 1.2.

plane location which corresponds to a given buckling mode is then treated as an additional degree of freedom in the process of minimizing the energy expression.

It should be noted that such a linear analysis is valid only under certain ideal circumstances. The most important of these are the requirements that the structural components under consideration experience only infinitesimal changes in geometry prior to buckling, and that sufficient symmetry is present that any assumptions aimed at uncoupling modes of deformation (in this case, the existence of neutral planes) are justified. In particular, sandwich panels of severely unbalanced face construction are likely to require a more rigorous (i. e., nonlinear) treatment than is presented here, since the range of validity of the assumptions concerning the neutral planes may be exceeded.

SECTION 2

THEORETICAL APPROACH

A displacement formulation is used to construct the total potential energy of the panel. The theory upon which this analysis is based is presented in Reference 12. The essential equations are cited here for completeness.

2.1 GEOMETRY

The panel configuration, reference axes and loading conventions are indicated in Figure 2. The x-y plane is chosen to coincide with the panel midplane. Positive senses of the stress resultants and displacements are as shown in the figure.

Figure 3 shows the assumed geometry of deformation in the xz coordinate plane. The displacement u_n represents an inplane deflection due to stretching only, and is not of interest here, since only the state of incipient buckling is to be considered. As the panel buckles, a transverse deflection occurs, accompanied by transverse shearing deformations within the core. During this deflection, it is assumed that in some plane located at $z = e_x$ there is no further inplane displacement, and that the rotations of the panel in the xz plane occur about points in this plane. Similarly in the yz plane, rotations are assumed to take place about the plane $z = e_y$. With this assumption, each of the inplane displacements of the panel are expressed in terms of the transverse deflection w and the core rotations ϕ and ψ .

2.2 BASIC EQUATIONS

The assumed geometry (Figure 3) permits the displacements of the core and faces to be stated as¹²

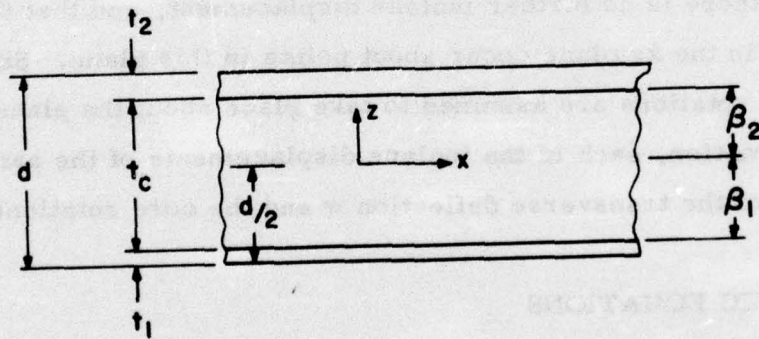
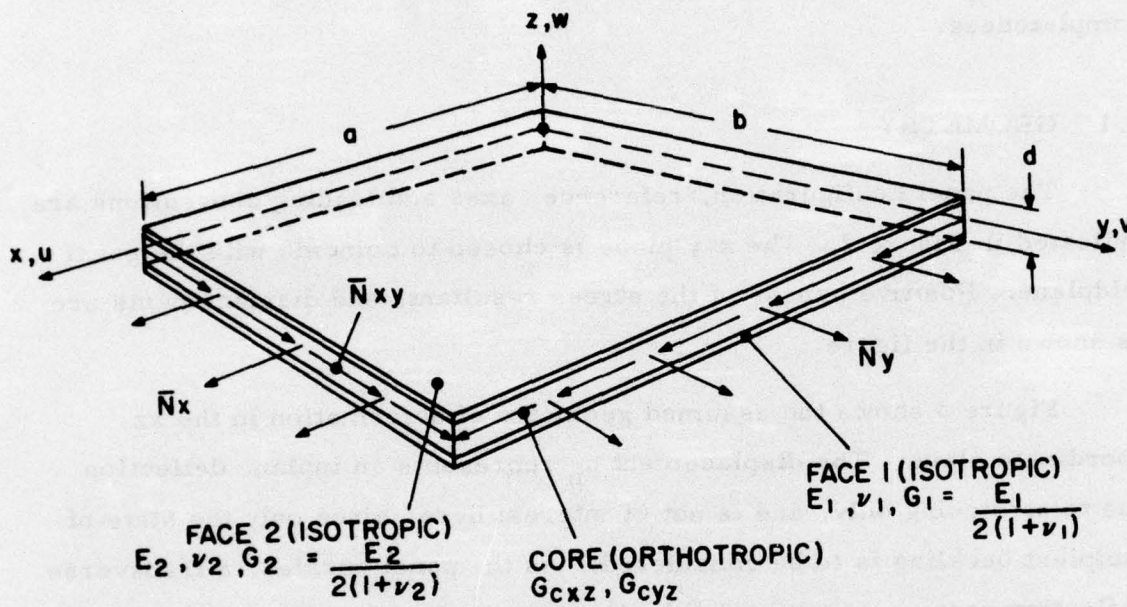


Figure 2. Panel Geometry.

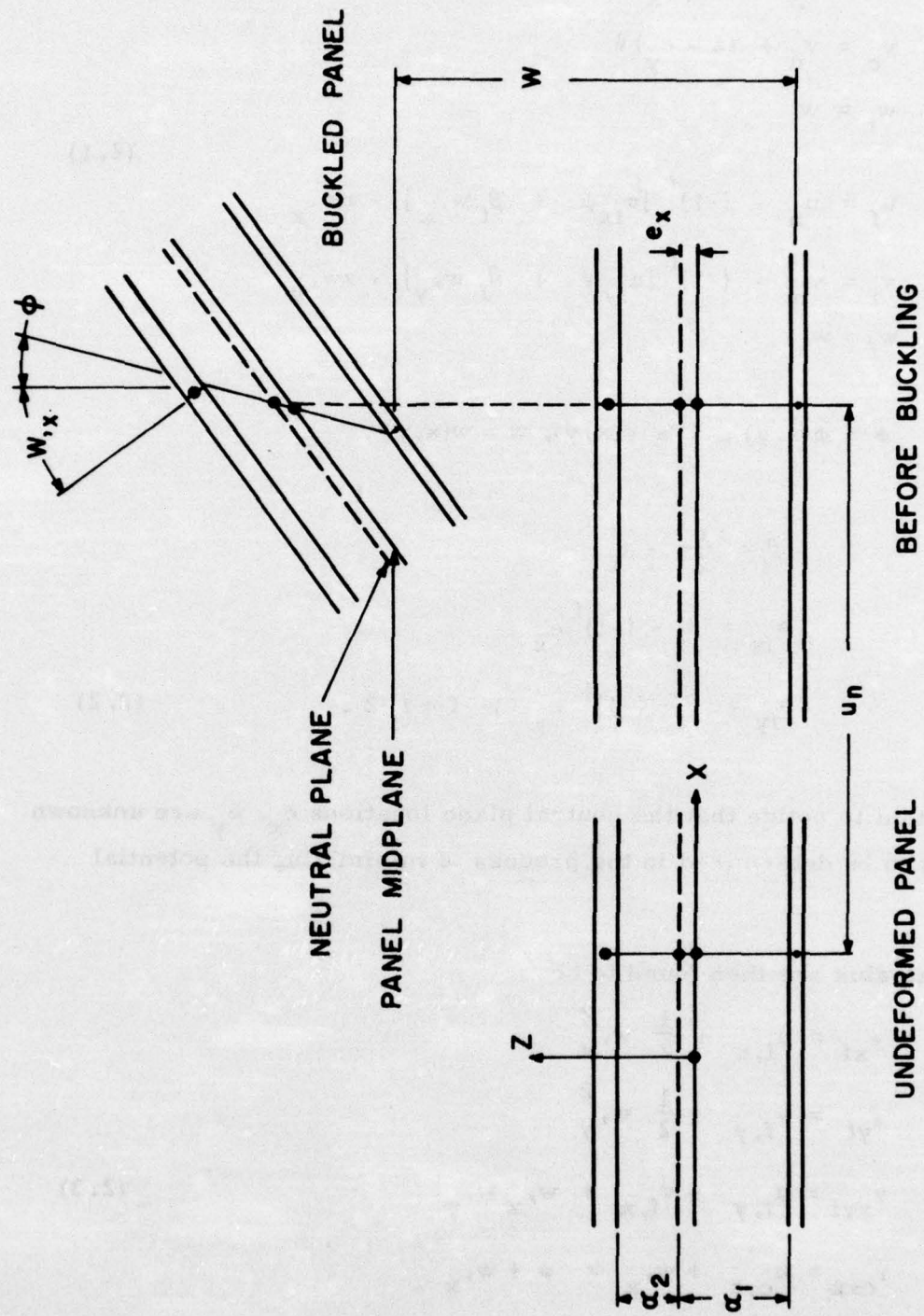


Figure 3. Geometry of Deformation in x - z Plane.

$$\begin{aligned}
 u_c &= u_n + (z - e_x) \phi \\
 v_c &= v_n + (z - e_y) \psi \\
 w_c &= w
 \end{aligned}
 \tag{2.1}$$

$$\begin{aligned}
 u_f &= u_n - (-1)^f [a_{fx} \phi + \beta_f w_{,x}] - zw_{,x} \\
 v_f &= v_n - (-1)^f [a_{fy} \psi + \beta_f w_{,y}] - zw_{,y} \\
 w_f &= w
 \end{aligned}$$

where

$$\phi = \phi(x, y), \quad \psi = \psi(x, y), \quad w = w(x, y),$$

and

$$\begin{aligned}
 \beta_f &= \frac{d}{2} - t_f \\
 a_{fx} &= \beta_f - (-1)^f e_x \\
 a_{fy} &= \beta_f - (-1)^f e_y \quad ; \quad f = 1, 2.
 \end{aligned}
 \tag{2.2}$$

It is important to notice that the neutral plane locations e_x , e_y are unknown parameters to be determined in the process of minimizing the potential energy.

The strains are then found to be

$$\begin{aligned}
 \epsilon_{xf} &= u_{f,x} + \frac{1}{2} w_{,x}^2 \\
 \epsilon_{yf} &= v_{f,y} + \frac{1}{2} w_{,y}^2 \\
 \gamma_{xyf} &= u_{f,y} + v_{f,x} + w_{,x} w_{,y} \\
 \gamma_{cxz} &= u_{c,z} + w_{,x} = \phi + w_{,x} \\
 \gamma_{cyz} &= v_{c,z} + w_{,y} = \psi + w_{,y}
 \end{aligned}
 \tag{2.3}$$

and the stresses by Hooke's law

$$\begin{aligned}\sigma_{xf} &= \frac{E_f}{1-\nu_f} (\epsilon_{xf} + \nu_f \epsilon_{yf}) \\ \sigma_{yf} &= \frac{E_f}{1-\nu_f} (\epsilon_{yf} + \nu_f \epsilon_{xf}) \\ \tau_{xyf} &= \frac{E_f}{2(1+\nu_f)} \gamma_{xyf} \\ \tau_{cxz} &= G_{cxz} \gamma_{cxz} \\ \tau_{cyz} &= G_{cyz} \gamma_{cyz}.\end{aligned}\tag{2.4}$$

It is evident that each of the components of displacement, strain and stress due to bending of the sandwich is a function only of the core rotations ϕ and ψ and the transverse displacement w . The responses due to inplane stretching are functions of the displacements u_n and v_n .

Notice in Equation 2.4 that the inplane stress resultants applied to the panel up to the point of incipient buckling are those related to the stretching deformations u_n and v_n ; that is,

$$\begin{aligned}\bar{N}_x &= \int_{-d/2}^{d/2} \frac{E}{1-\nu} (u_{n,x} + \nu v_{n,y}) dz \\ \bar{N}_{xy} &= \int_{-d/2}^{d/2} \frac{E}{2(1+\nu)} (u_{n,y} + \nu u_{n,x}) dz \\ \bar{N}_y &= \int_{-d/2}^{d/2} \frac{E}{1-\nu} (\nu u_{n,x} + v_{n,y}) dz\end{aligned}\tag{2.5}$$

Since the core does not resist inplane stretching, these integrals receive nonzero contributions only from the face sheets. Accordingly, each of the resultants defined by Equation 2.5 may be thought of as the sum of the stress resultants in the two facings; that is,

$$\begin{aligned}\bar{N}_x &= \bar{N}_{x1} + \bar{N}_{x2} \\ \bar{N}_y &= \bar{N}_{y1} + \bar{N}_{y2} \\ \bar{N}_{xy} &= \bar{N}_{xy1} + \bar{N}_{xy2}.\end{aligned}\tag{2.6}$$

2.3 POTENTIAL ENERGY

The total potential energy of the panel may be expressed as¹⁴

$$\begin{aligned}\pi_p &= \frac{1}{2} \sum_{f=1}^2 \iiint_{V_f} \left[\sigma_{xf} \epsilon_{xf} + \tau_{xyf} \gamma_{xyf} + \sigma_{yf} \epsilon_{yf} \right. \\ &\quad \left. + \frac{1}{t_f} \left(\bar{N}_{xf} w_{,x}^2 + 2 \bar{N}_{xyf} w_{,x} w_{,y} + \bar{N}_{yf} w_{,y}^2 \right) \right] dx dy dz \\ &\quad + \frac{1}{2} \iiint_{V_c} (\tau_{cxz} \gamma_{cxz} + \tau_{cyz} \gamma_{cyz}) dx dy dz\end{aligned}\tag{2.7}$$

where f denotes the respective face sheets, and V_f and V_c represent the volumes of the facings and the core, respectively. In the statement of Equation 2.7, it is tacitly assumed that displacements experienced at points within the panel prior to buckling are negligible (that is, $u_n = v_n = 0$). The stress resultants \bar{N}_{xf} , \bar{N}_{xyf} , \bar{N}_{yf} have, therefore, assumed the character of initial stresses present throughout the face sheets immediately preceding the time of buckling. Furthermore, the stresses σ_{ijf} and the strains ϵ_{ijf} are to be interpreted as departures from the prebuckled equilibrium state

defined by the displacements u_n and v_n . It should also be noted that the squares of the derivatives of the inplane displacements have been neglected in comparison with the squares of the slopes;* that is,

$$(u_{f,x}^2; u_{f,y}^2; v_{f,x}^2; v_{f,y}^2) \ll (w_{,x}^2; w_{,y}^2) \quad (2.8)$$

The displacement formulation corresponding to Equation 2.7 is obtained with the use of Equations 2.3 and 2.4. It is then assumed, for the linearized problem, that cubic and quartic terms in the strain energy may be neglected. After making this substitution and performing the integrations through the thickness of the panel, the following potential energy functional is obtained:**

$$\begin{aligned} \pi_P = & \frac{1}{2} \sum_{f=1}^2 \frac{E_f}{\lambda_f} \int_0^b \int_0^a \left\{ \alpha_{fx}^2 t_f \left(\phi_{,x}^2 + \frac{1-\nu_f}{2} \phi_{,y}^2 \right) \right. \\ & + \alpha_{fx} \alpha_{fy} t_f \left[2\nu_f \phi_{,x} \psi_{,y} + (1-\nu_f) \phi_{,y} \psi_{,x} \right] \\ & + \alpha_{fy}^2 t_f \left(\psi_{,y}^2 + \frac{1-\nu_f}{2} \psi_{,x}^2 \right) \\ & - \alpha_{fx} t_f^2 \left[\phi_{,x} (w_{,xx} + \nu_f w_{,yy}) + (1-\nu_f) \phi_{,y} w_{,xy} \right] \\ & - \alpha_{fy} t_f^2 \left[\psi_{,y} (w_{,yy} + \nu_f w_{,xx}) + (1-\nu_f) \psi_{,x} w_{,xy} \right] \\ & \left. + \frac{1}{3} t_f^3 \left[w_{,xx}^2 + 2\nu_f w_{,xx} w_{,yy} + w_{,yy}^2 + 2(1-\nu_f) w_{,xy}^2 \right] \right\} dx dy \end{aligned}$$

* This assumption is reflected in Equation 2.3.

** The definition $\lambda_f = 1 - \nu_f^2$ has been introduced here.

$$\begin{aligned}
& + \frac{1}{2} \int_0^b \int_0^a \left[G_{cxz} t_c (\phi + w_{,x})^2 + G_{cyz} t_c (\psi + w_{,y})^2 \right] dx dy \\
& + \frac{1}{2} \int_0^b \int_0^a \left[\bar{N}_x w_{,x}^2 + 2\bar{N}_{xy} w_{,x} w_{,y} + \bar{N}_y w_{,y}^2 \right] dx dy \quad (2.9)
\end{aligned}$$

It is important to realize that, although the resultants \bar{N}_x , \bar{N}_{xy} , \bar{N}_y are required to satisfy equilibrium before buckling, they need not be constants throughout the panel. Hence, the quantities \bar{N}_x and \bar{N}_y may be taken to include both uniform and linearly varying compressive forces; that is,

$$\begin{aligned}
\bar{N}_x &= \bar{N}_{x0} + \bar{N}_{xb}(y/b) \\
\bar{N}_y &= \bar{N}_{y0} + \bar{N}_{yb}(x/a).
\end{aligned} \quad (2.10)$$

These forms for the applied loads satisfy the equations of equilibrium,

$$\begin{aligned}
N_{x,x} + N_{xy,y} &= 0 \\
N_{xy,x} + N_{y,y} &= 0,
\end{aligned}$$

and permit the consideration of edgewise bending forces. The special case of a pure edgewise bending moment (see Figure 1) will be indicated by the symbols \bar{N}_{xB} or \bar{N}_{yB} , such that

$$\begin{aligned}
\bar{N}_x &= \bar{N}_{xB}(1-2y/b) \\
\bar{N}_y &= \bar{N}_{yB}(1-2x/a).
\end{aligned} \quad (2.11)$$

That is, the linearly varying component of the pure edgewise bending load is twice the magnitude of the uniform component, and opposite in sign.

SECTION 3

NUMERICAL SOLUTION FOR BUCKLING LOADS

The principle of minimum potential energy can now be applied to produce the conditions of equilibrium. The potential energy is expressed in terms of a complete and geometrically admissible set of functions. Application of the principle of minimum potential energy produces the approximate minimizing relations, in the form of an eigenvalue problem. By considering successively larger solution spaces, each of which contains the previous one, monotonic convergence to the solution is guaranteed.

3.1 DISCRETIZATION OF THE POTENTIAL ENERGY BY THE RITZ METHOD

The total potential energy associated with the incipient buckling of the panel is given by Equation 2.9 in terms of w , ϕ and ψ . Admissible assumed-mode functions must satisfy conditions of continuity and differentiability, as well as the imposed boundary conditions¹² for simple supports,

$$w(0, y) = w(a, y) = w(x, 0) = w(x, b) = 0;$$

therefore an appropriate set of functions is

$$\begin{aligned} w(x, y) &= \sum_{m=1}^{\ell} \sum_{n=1}^{\ell} W_{mn} \sin \frac{m\pi x}{a} \sin \frac{n\pi y}{b} \\ \phi(x, y) &= \sum_{m=1}^{\ell} \sum_{n=1}^{\ell} \phi_{mn} \cos \frac{m\pi x}{a} \sin \frac{n\pi y}{b} \\ \psi(x, y) &= \sum_{m=1}^{\ell} \sum_{n=1}^{\ell} \psi_{mn} \sin \frac{m\pi x}{a} \cos \frac{n\pi y}{b} . \end{aligned} \quad (3.1)$$

Substitution of the assumed forms of the displacements into the potential energy (Equation 2.9) yields a functional π_p which is expressed entirely in terms of the trigonometric functions of Equation 3.1. The integrations over the area may then be carried out directly, according to the following formulas:

$$\int_0^a \sin \frac{m\pi x}{a} \sin \frac{r\pi x}{a} dx = \frac{a}{2} \delta_{mr}$$

$$\int_0^a \cos \frac{m\pi x}{a} \cos \frac{r\pi x}{a} dx = \frac{a}{2} \delta_{mr}$$

$$\int_0^a \sin \frac{m\pi x}{a} \cos \frac{r\pi x}{a} dx = \frac{2am}{\pi(m^2 - r^2)} \Delta_{mr}$$

$$\int_0^a x \sin \frac{m\pi x}{a} \sin \frac{r\pi x}{a} dx = \frac{a^2}{4} \delta_{mr} - \frac{4a^2 mr}{\pi^2 (m^2 - r^2)^2} \Delta_{mr}$$

where δ_{mr} is the Kronecker delta, and Δ_{mr} is defined such that for any arithmetic expression* denoted by X,

$$X \Delta_{mr} = \begin{cases} 0 & ; m+r \text{ even} \\ X & ; m+r \text{ odd} \end{cases}$$

The expression obtained for the potential energy upon substituting the assumed modes (Equations 3.1) and performing the indicated integrations is given by

*The expression may be indefinite or definite.

$$\begin{aligned}
\pi_p = & \sum_{m=1}^{\ell} \sum_{n=1}^{\ell} \left\{ \sum_{f=1}^2 \frac{E_f t_f}{2 \lambda_f} \left(\alpha_{fxmn}^2 \left[\frac{m^2 \pi^2}{a^2} + \left(\frac{1-\nu_f}{2} \right) \frac{n^2 \pi^2}{b^2} \right] \Phi_{mn}^2 \right. \right. \\
& + \alpha_{fxmn} \alpha_{fy mn} (1 + \nu_f) \frac{mn \pi^2}{ab} \Phi_{mn} \Psi_{mn} \\
& + \alpha_{fymn}^2 \left[\frac{n^2 \pi^2}{b^2} + \left(\frac{1-\nu_f}{2} \right) \frac{m^2 \pi^2}{a^2} \right] \Psi_{mn}^2 \\
& - t_f \alpha_{fxmn} \left(\frac{m^3 \pi^3}{a^3} + \frac{mn^2 \pi^3}{ab^2} \right) W_{mn} \Phi_{mn} \\
& - t_f \alpha_{fymn} \left(\frac{n^3 \pi^3}{b^3} + \frac{m^2 n \pi^3}{a^2 b} \right) W_{mn} \Psi_{mn} \\
& \left. + \frac{1}{3} t_f^2 \left(\frac{m^2 \pi^2}{a^2} + \frac{n^2 \pi^2}{b^2} \right)^2 W_{mn}^2 \right) \\
& + \frac{1}{2} G_{cxz} t_c \left[\Phi_{mn} + \frac{m \pi}{a} W_{mn} \right]^2 + \frac{1}{2} G_{cyz} t_c \left[\Psi_{mn} + \frac{n \pi}{b} W_{mn} \right]^2 \\
& + \left(\frac{1}{2} \bar{N}_{x0} \frac{m^2 \pi^2}{a^2} + \frac{1}{2} \bar{N}_{y0} \frac{n^2 \pi^2}{b^2} \right) W_{mn}^2 \\
& + \frac{\bar{N}_{xy}}{ab} \sum_{r=1}^{\ell} \sum_{s=1}^{\ell} \frac{16mnr s}{(r^2 - m^2)(n^2 - s^2)} \Delta_{mr} \Delta_{ns} W_{mn} W_{rs} \left. \right] \frac{ab}{4} \\
& + \frac{1}{2} \bar{N}_{xb} \frac{m^2 \pi^2}{ab} \sum_{s=1}^{\ell} \left[\frac{b^2}{8} \delta_{ns} - \frac{2b^2 ns}{\pi^2 (n^2 - s^2)} \Delta_{ns} \right] W_{mn} W_{ms} \\
& + \frac{1}{2} \bar{N}_{yb} \frac{n^2 \pi^2}{ab} \sum_{r=1}^{\ell} \left[\frac{a^2}{8} \delta_{mr} - \frac{2a^2 mr}{\pi^2 (m^2 - r^2)} \Delta_{mr} \right] W_{mn} W_{rr} \left. \right\}. \quad (3.2)
\end{aligned}$$

It is important to recognize that since the parameters α_{fx} , α_{fy} contain the positions of the neutral planes (Equation 2.2), they too are undetermined parameters dependent upon the particular buckling mode; that is,

$$\alpha_{fx} = (\alpha_{fx})_{mn}$$

$$\alpha_{fy} = (\alpha_{fy})_{mn}.$$

Since the energy expression contains cubic terms (such as $\alpha_{fxmn} \phi_{mn}^2$) which are not quadratic forms in the unknowns ϕ_{mn} , ψ_{mn} , W_{mn} , e_{xmn} and e_{ymn} , the minimization of the energy in its present form will involve the solution of a system of nonlinear simultaneous equations. In order to circumvent this difficulty, it is advantageous to define the additional parameters

$$h_{mn} = e_{xmn} \phi_{mn}$$

$$k_{mn} = e_{ymn} \psi_{mn}.$$

It is also convenient to define a (4 x 4) matrix A, a (4 x 1) vector B, and a constant C corresponding to each mode, as follows:

$$a_{11} = \sum_{f=1}^2 \frac{E_f}{\lambda_f} t_f \beta_f^2 \left[\frac{m^2 \pi^2}{a^2} + \frac{1-\nu_f}{2} \frac{n^2 \pi^2}{b^2} \right] + G_{cxz} t_c$$

$$a_{12} = \sum_{f=1}^2 \frac{1}{2} \frac{E_f}{\lambda_f} t_f \beta_f^2 (1 + \nu_f) \frac{mn\pi^2}{ab}$$

$$a_{13} = \sum_{f=1}^2 \frac{E_f}{\lambda_f} t_f (-1)^{f+1} \beta_f \left[\frac{m^2 \pi^2}{a^2} + \frac{1-\nu_f}{2} \frac{n^2 \pi^2}{b^2} \right]$$

$$a_{14} = \sum_{f=1}^2 \frac{1}{2} \frac{E_f}{\lambda_f} t_f \beta_f (-1)^{f+1} (1 + \nu_f) \frac{mn\pi^2}{ab}$$

$$a_{21} = a_{12}$$

$$a_{22} = \sum_{f=1}^2 \frac{E_f}{\lambda_f} t_f \beta_f^2 \left[\frac{n^2 \pi^2}{b^2} + \frac{1 - \nu_f}{2} \frac{m^2 \pi^2}{a^2} \right] + G_{cyz} t_c$$

$$a_{23} = a_{14}$$

$$a_{24} = \sum_{f=1}^2 \frac{E_f}{\lambda_f} t_f (-1)^{f+1} \beta_f \left[\frac{n^2 \pi^2}{b^2} + \frac{1 - \nu_f}{2} \frac{m^2 \pi^2}{a^2} \right]$$

$$a_{31} = a_{13}$$

$$a_{32} = a_{23}$$

$$a_{33} = \sum_{f=1}^2 \frac{E_f}{\lambda_f} t_f \left[\frac{m^2 \pi^2}{a^2} + \frac{1 - \nu_f}{2} \frac{n^2 \pi^2}{b^2} \right]$$

$$a_{34} = \sum_{f=1}^2 \frac{1}{2} \frac{E_f}{\lambda_f} t_f (1 + \nu_f) \frac{m n \pi^2}{ab}$$

$$a_{41} = a_{14}$$

$$a_{42} = a_{24}$$

$$a_{43} = a_{34}$$

$$a_{44} = \sum_{f=1}^2 \frac{E_f}{\lambda_f} t_f \left[\frac{n^2 \pi^2}{b^2} + \frac{1 - \nu_f}{2} \frac{m^2 \pi^2}{a^2} \right]$$

$$\begin{aligned}
b_1 &= \sum_{f=1}^2 -\frac{1}{2} \frac{E_f}{\lambda_f} t_f^2 \beta_f \left[\frac{m^3 \pi^3}{a^3} + \frac{mn^2 \pi^3}{ab^2} \right] + G_{cxz} t_c \frac{m\pi}{a} \\
b_2 &= \sum_{f=1}^2 -\frac{1}{2} \frac{E_f}{\lambda_f} t_f^2 \beta_f \left[\frac{n^3 \pi^3}{b^3} + \frac{m^2 n \pi^3}{a^2 b} \right] + G_{cyz} t_c \frac{n\pi}{b} \\
b_3 &= \sum_{f=1}^2 \frac{1}{2} \frac{E_f}{\lambda_f} t_f^2 (-1)^f \left[\frac{m^3 \pi^3}{a^3} + \frac{mn^2 \pi^3}{ab^2} \right] \\
b_4 &= \sum_{f=1}^2 \frac{1}{2} \frac{E_f}{\lambda_f} t_f^2 (-1)^f \left[\frac{n^3 \pi^3}{b^3} + \frac{m^2 n \pi^3}{a^2 b} \right] \\
C &= \sum_{f=1}^2 \frac{E_f}{\lambda_f} \frac{t_f^3}{3} \left(\frac{m^2 \pi^2}{a^2} + \frac{n^2 \pi^2}{b^2} \right) + G_{cxz} t_c \frac{m^2 \pi^2}{a^2} \\
&\quad + G_{cyz} t_c \frac{n^2 \pi^2}{b^2} .
\end{aligned}$$

With these conventions and the use of Equation 2.2, the potential energy (Equation 3.2) can be written in the form

$$\pi'_p = \frac{4}{ab} \pi_p = \sum_{m=1}^l \sum_{n=1}^l \left(\frac{1}{2} \left\{ \begin{array}{c} \Phi_{mn} \\ \Psi_{mn} \\ h_{mn} \\ k_{mn} \\ \dots \\ W_{mn} \end{array} \right\}^T \left[\begin{array}{cccc|cccc} a_{11} & a_{12} & a_{13} & a_{14} & b_1 & & & \\ a_{12} & a_{22} & a_{23} & a_{24} & b_2 & & & \\ a_{13} & a_{23} & a_{33} & a_{34} & b_3 & & & \\ a_{14} & a_{24} & a_{34} & a_{44} & b_4 & & & \\ \dots & & & & & & & \\ b_1 & b_2 & b_3 & b_4 & C & & & \end{array} \right] \left\{ \begin{array}{c} \Phi_{mn} \\ \Psi_{mn} \\ h_{mn} \\ k_{mn} \\ \dots \\ W_{mn} \end{array} \right\} \right)$$

$$\begin{aligned}
& + \frac{1}{2} \left[\bar{N}_{x_0} \frac{m^2 \pi^2}{a^2} + \bar{N}_{y_0} \frac{n^2 \pi^2}{b^2} \right] W_{mn}^2 \\
& + \frac{1}{2} \bar{N}_{xy} \sum_{r=1}^l \sum_{s=1}^l \frac{32}{ab} \frac{mnr s}{(m^2 - r^2)(s^2 - n^2)} \Delta_{mr} \Delta_{ns} W_{mn} W_{rs} \\
& + \frac{1}{2} \bar{N}_{xb} \frac{4m^2 \pi^2}{a^2 b^2} \sum_{s=1}^l \left[\frac{b^2}{8} \delta_{ns} - \frac{2b^2 ns}{\pi^2 (n^2 - s^2)^2} \Delta_{ns} \right] W_{mn} W_{ms} \\
& + \frac{1}{2} \bar{N}_{yb} \frac{4n^2 \pi^2}{a^2 b^2} \sum_{r=1}^l \left[\frac{a^2}{8} \delta_{mr} - \frac{2a^2 mr}{\pi^2 (m^2 - r^2)^2} \Delta_{mr} \right] W_{mn} W_{rn} \Big). \quad (3.3)
\end{aligned}$$

The discretized potential energy (Equation 3.3) is a quadratic function of the undetermined parameters Φ_{mn} , Ψ_{mn} , h_{mn} , k_{mn} , and W_{mn} . The use of the principle of minimum potential energy then leads to a linear system of equations for the undetermined parameters.

3.2 APPLICATION OF THE PRINCIPLE OF MINIMUM POTENTIAL ENERGY

The variational form of the principle of minimum potential energy is

$$\delta \pi_p = 0,$$

where π_p is given in Equation 2.9. After discretization using the Ritz method, the minimum potential energy principle requires

$$\frac{\partial}{\partial p_i} \left[\pi_p(p_1, p_2, \dots, p_n) \right] = 0; \quad i=1, 2, \dots, n,$$

where the p_i are unknown discrete parameters. For the present case, from Equation 3.3,

$$\begin{Bmatrix} \partial \pi'_p / \partial \Phi_{mn} \\ \partial \pi'_p / \partial \Psi_{mn} \\ \partial \pi'_p / \partial h_{mn} \\ \partial \pi'_p / \partial k_{mn} \end{Bmatrix} = \begin{bmatrix} a_{11} & a_{12} & a_{13} & a_{14} & \vdots & b_1 \\ a_{12} & a_{22} & a_{23} & a_{24} & \vdots & b_2 \\ a_{13} & a_{23} & a_{33} & a_{34} & \vdots & b_3 \\ a_{14} & a_{24} & a_{34} & a_{44} & \vdots & b_4 \end{bmatrix}_{mn} \begin{Bmatrix} \Phi_{mn} \\ \Psi_{mn} \\ h_{mn} \\ k_{mn} \\ W_{mn} \end{Bmatrix} = \begin{Bmatrix} 0 \\ 0 \\ 0 \\ 0 \end{Bmatrix} \quad (3.4)$$

$$\begin{aligned} \text{and } \partial \pi'_p / \partial W_{mn} &= (b_{1mn} \Phi_{mn} + b_{2mn} \Psi_{mn} + b_{3mn} h_{mn} + b_{4mn} k_{mn} + C_{mn} W_{mn}) \\ &+ \left(\bar{N}_{x0} \frac{m^2 \pi^2}{a^2} + \bar{N}_{y0} \frac{n^2 \pi^2}{b^2} \right) W_{mn} \\ &+ \bar{N}_{xy} \sum_{r=1}^l \sum_{s=1}^l \frac{32}{ab} \frac{mnr s}{(m^2 - r^2)(s^2 - n^2)} \Delta_{mr} \Delta_{ns} W_{rs} \\ &+ 4\bar{N}_{xb} \frac{m^2 \pi^2}{a^2} \sum_{s=1}^l \left[\frac{1}{8} \delta_{ns} - \frac{2ns}{\pi^2 (n^2 - s^2)^2} \Delta_{ns} \right] W_{ms} \\ &+ 4\bar{N}_{yb} \frac{n^2 \pi^2}{b^2} \sum_{r=1}^l \left[\frac{1}{8} \delta_{mr} - \frac{2mr}{\pi^2 (m^2 - r^2)^2} \Delta_{mr} \right] W_{rn} = 0. \quad (3.5) \end{aligned}$$

The unknown parameters may be normalized with respect to W_{mn} by taking

$$\begin{aligned} X_1 &= \Phi_{mn} / W_{mn} & ; & & X_2 &= \Psi_{mn} / W_{mn} \\ X_3 &= h_{mn} / W_{mn} & ; & & X_4 &= k_{mn} / W_{mn} . \end{aligned}$$

Upon substituting these definitions in Equations 3.4 and 3.5, the following final system of equations is obtained:

$$\begin{bmatrix} a_{11} & a_{12} & a_{13} & a_{14} \\ a_{12} & a_{22} & a_{23} & a_{24} \\ a_{13} & a_{23} & a_{33} & a_{34} \\ a_{14} & a_{24} & a_{34} & a_{44} \end{bmatrix}_{mn} \begin{Bmatrix} X_1 \\ X_2 \\ X_3 \\ X_4 \end{Bmatrix}_{mn} + \begin{Bmatrix} b_1 \\ b_2 \\ b_3 \\ b_4 \end{Bmatrix}_{mn} = \begin{Bmatrix} 0 \\ 0 \\ 0 \\ 0 \end{Bmatrix}, \quad (3.6)$$

and

$$\begin{aligned} & (C_{mn} + \sum_{j=1}^4 b_{jmn} X_{jmn}) W_{mn} + \left[\bar{N}_{x_0} \frac{m^2 \pi^2}{a^2} + N_{y_0} \frac{n^2 \pi^2}{b^2} \right] W_{mn} \\ & + \bar{N}_{xy} \sum_{r=1}^l \sum_{s=1}^l \frac{32}{ab} \frac{mnr s}{(m^2 - r^2)(s^2 - n^2)} \Delta_{mr} \Delta_{ns} W_{rs} \\ & + 4\bar{N}_{xb} \frac{m^2 \pi^2}{a^2} \sum_{s=1}^l \left[\frac{1}{8} \delta_{ns} - \frac{2ns}{\pi^2 (n^2 - s^2)^2} \Delta_{ns} \right] W_{ms} \\ & + 4\bar{N}_{yb} \frac{n^2 \pi^2}{b^2} \sum_{r=1}^l \left[\frac{1}{8} \delta_{mr} - \frac{2mr}{\pi^2 (m^2 - r^2)^2} \Delta_{mr} \right] W_{rn} = 0; \\ & \qquad \qquad \qquad m = 1, 2, \dots, l \\ & \qquad \qquad \qquad n = 1, 2, \dots, l. \end{aligned} \quad (3.7)$$

3.3 ASSEMBLY OF EQUATIONS FOR SOLUTION

It is clear from Equations 3.6 and 3.7 that only the parameters W_{mn} must be considered explicitly in the solution process, since Equation 3.6 can be inverted to obtain the X_i . The quantities W_{mn} are collected in a vector,

$$\{W\}^T = [w_{11}, w_{12}, \dots, w_{1l}, w_{21}, w_{22}, \dots, w_{2l}, \dots, w_{l1}, w_{l2}, \dots, w_{ll}].$$

The prescribed loads are assigned constant relative magnitudes, and are related to a single factor which is sufficient to indicate their intensity; that is,

$$(\bar{N}_{xo}, \bar{N}_{xb}, \bar{N}_{xy}, \bar{N}_{yb}, \bar{N}_{yo}) = \lambda (n_{xo}, n_{xb}, n_{xy}, n_{yb}, n_{yo}).$$

Equations 3.7 can then be arranged in the form

$$\begin{bmatrix} K \\ \ell^2 \times \ell^2 \end{bmatrix} \begin{Bmatrix} W \\ \ell^2 \times 1 \end{Bmatrix} + \lambda \begin{bmatrix} G \\ \ell^2 \times \ell^2 \end{bmatrix} \begin{Bmatrix} W \\ \ell^2 \times 1 \end{Bmatrix} = \begin{Bmatrix} 0 \\ \end{Bmatrix}. \quad (3.8)$$

Here the matrix K is diagonal, with the i^{th} diagonal entry defined by

$$k_{ii} = C_{mn} + \sum_{j=1}^4 b_{jmn} X_{jmn},$$

where

$$i = \ell(m-1) + n$$

and the X_j are solutions of Equation 3.6 for the appropriate m and n. The i, j^{th} entry of the matrix G is related to the applied loads terms in Equations 3.7, such that

$$\begin{aligned} g_{ij} = & \left[n_{xo} \frac{m^2 \pi^2}{a^2} + n_{yo} \frac{n^2 \pi^2}{b^2} \right] \delta_{mr} \delta_{ns} \\ & + n_{xy} \frac{32}{ab} \frac{1}{(m^2 - r^2)(s^2 - n^2)} \Delta_{mr} \Delta_{ns} \\ & + 4n_{xb} \frac{m^2 \pi^2}{a^2} \delta_{mr} \left[\frac{1}{8} \delta_{ns} - \frac{2ns}{\pi^2 (n^2 - s^2)^2} \Delta_{ns} \right] \\ & + 4n_{yb} \frac{n^2 \pi^2}{b^2} \delta_{ns} \left[\frac{1}{8} \delta_{mr} - \frac{2mr}{\pi^2 (m^2 - r^2)^2} \Delta_{mr} \right], \end{aligned}$$

where

$$i = l(m-1) + n$$

and

$$j = l(r-1) + s .$$

Finally, the critical loads and corresponding mode shapes of the panel are obtained by solving the eigenvalue problem represented by Equation 3.8.

SECTION 4

SUMMARY OF RESULTS

The procedure outlined in Section 3 has been implemented in a computer program. Numerical results have been obtained for numerous examples of individual critical loads from other sources in order to verify its accuracy. Critical loads have also been calculated for various cases of combined loadings, and compared with existing interaction formulas.

4.1 VERIFICATION EXAMPLES

The results of typical calculations performed in the process of verifying the computer program are presented in Table 1. The example cited from Reference 15 is based upon a nonlinear, post buckling finite element analysis. The remainder are taken from linear buckling analyses similar to that presented here. Note that Examples 4, 5, 6, and 11 are specializations of the theory to the case of a classical isotropic plate.

Agreement with the previously published results was good in all cases. Critical loads calculated for compression agree closely with those cited, since the various modes uncouple, allowing the equations to be solved in closed form.

Pure edgewise bending^{*} results are also in good agreement with the previous values. Convergence for these calculations generally requires no more than 6 terms in the displacement series (Equation 3.1). The results cited from Reference 10 apply for face sheets having only membrane stiffness. Consequently the present analysis yields a slightly higher critical load for Example 9.

* Pure edgewise bending values are stated in the form of Equations 2.11; that is, the value of N_{xB} defines $\bar{N}_x = \bar{N}_{xB} (1 - 2y/b)$, and so on.

TABLE 1: VERIFICATION RESULTS FOR INDIVIDUAL CRITICAL LOADS

No.	Construction	Loading	E_1 E_2	ν_1 ν_2	t_1 t_2	G_{cxz} G_{cyz}	t_c	a b	Terms in Series	Critical Loads	Ref.	Reference Result
1	Sandwich	Compr.	9.5×10^6 9.5×10^6	.30 .30	.021 .021	19000. 19000.	.181	23.5 23.5	1	$N_x = -309.39$	15	-307.5
2	Sandwich	Compr.	10.6×10^6 10.6×10^6	.30 .30	.025 .025	50000. 20000	.25	20. 20.	1	$N_x = -1025.7$	1	-1025.7
3	Sandwich	Compr.	10.6×10^6 10.6×10^6	.30 .30	.025 .025	50000 20000	.25	60. 20.	3	$N_x = -1025.7$	1	-1025.7
4	Isotropic	Compr.	10.6×10^6 10.6×10^6	.30 .30	.25 .25	= =	0.	20. 20.	1	$N_x = -11975$	16	-11975
5	Isotropic	Shear	10.6×10^6 10.6×10^6	.30 .30	.25 .25	= =	0.	20. 20.	7	$N_{xy} = 27931$	16	27963
6	Isotropic	Shear	10.6×10^6 10.6×10^6	.30 .30	1/6 1/6	= =	0.	17. 17.	7	$N_{xy} = 11455$	16	11468
7	Sandwich	Shear	10.6×10^6 10.6×10^6	.25 .25	.025 .025	4359. 4359.	.25	10. 40.	10	$N_{xy} = 1344.3$	7	1349.2
8	Sandwich	Shear	10.6×10^6 $15. \times 10^6$.25 .25	.020 .015	5496. 5496.	.1875	7. 28.	10	$N_{xy} = 1252.7$	7	1260.5
9	Sandwich	Bending	10.6×10^6 10.6×10^6	.25 .25	.005 .005	4359. 4359.	.25	24. 40.	6	$N_{xB}^* = 258.7$	10	256.1
10	Sandwich	Bending	10.2×10^6 10.2×10^6	.30 .30	.005 .005	540.8 540.8	.225	48. 48.	6	$N_{xB} = 119.3$	1	119.8
11	Isotropic	Bending	10.0×10^6 10.0×10^6	.30 .30	.0625 .0625	= =	.0	40. 60.	6	$N_{xB} = 117.1$	16	116.7

* Maximum value along edge is given here; i. e., $\bar{N}_x = N_{xB}(1-2y/b)$.

Comparison of the calculations for pure edgewise shear loads show much larger discrepancies than for bending or compression. This is to be expected, since convergence to the critical shear load is quite slow due to the marked difference between the forms of the assumed displacements and the true mode shapes. Slightly lower values are obtained for each example by the present method. These results appear to be more accurate than the previously published values, since more terms in the displacement series (Equations 3.1) are considered, and because the solution does not depend upon discarding various terms from the complete series, as has been done in Reference 7.

4.2 TYPICAL RESULTS FOR COMBINED LOADINGS

Critical loads calculations for typical sandwich panels subjected to combined loadings are presented in Figures 4 and 5. The physical data for each of the three panels considered is listed in Table 2. Panel 1 is square, with balanced facings and equal shear moduli in the core. Panel 2 is similar to Panel 1, but rectangular ($a/b = .556$). The third panel studied is rectangular with unequal core shear moduli.

The effect of edgewise shear loading upon the magnitude of the critical compressive loads is plotted in Figure 4. Here $\bar{N}_{x0} = \bar{N}_{y0}$ for all points calculated, while the magnitude of the applied shear load is increased relative to the compressive forces. Results are given in terms of the ratio

$$\frac{\bar{N}_{xcr}}{\bar{N}_{xcr}^*} = \frac{\text{Actual critical compressive load}}{\text{Critical compressive load for } \bar{N}_{xy} = 0}$$

and the relative magnitude of the shear and compressive stress, \bar{N}_{xy}/\bar{N}_x .

Figure 5 depicts the effect of the addition of edgewise bending moments to an applied biaxial loading. In each case the compressive loadings \bar{N}_{x0} , \bar{N}_{y0} are equal. A shear load is also applied such that $\bar{N}_{xy} = 2\bar{N}_{x0}$. Various

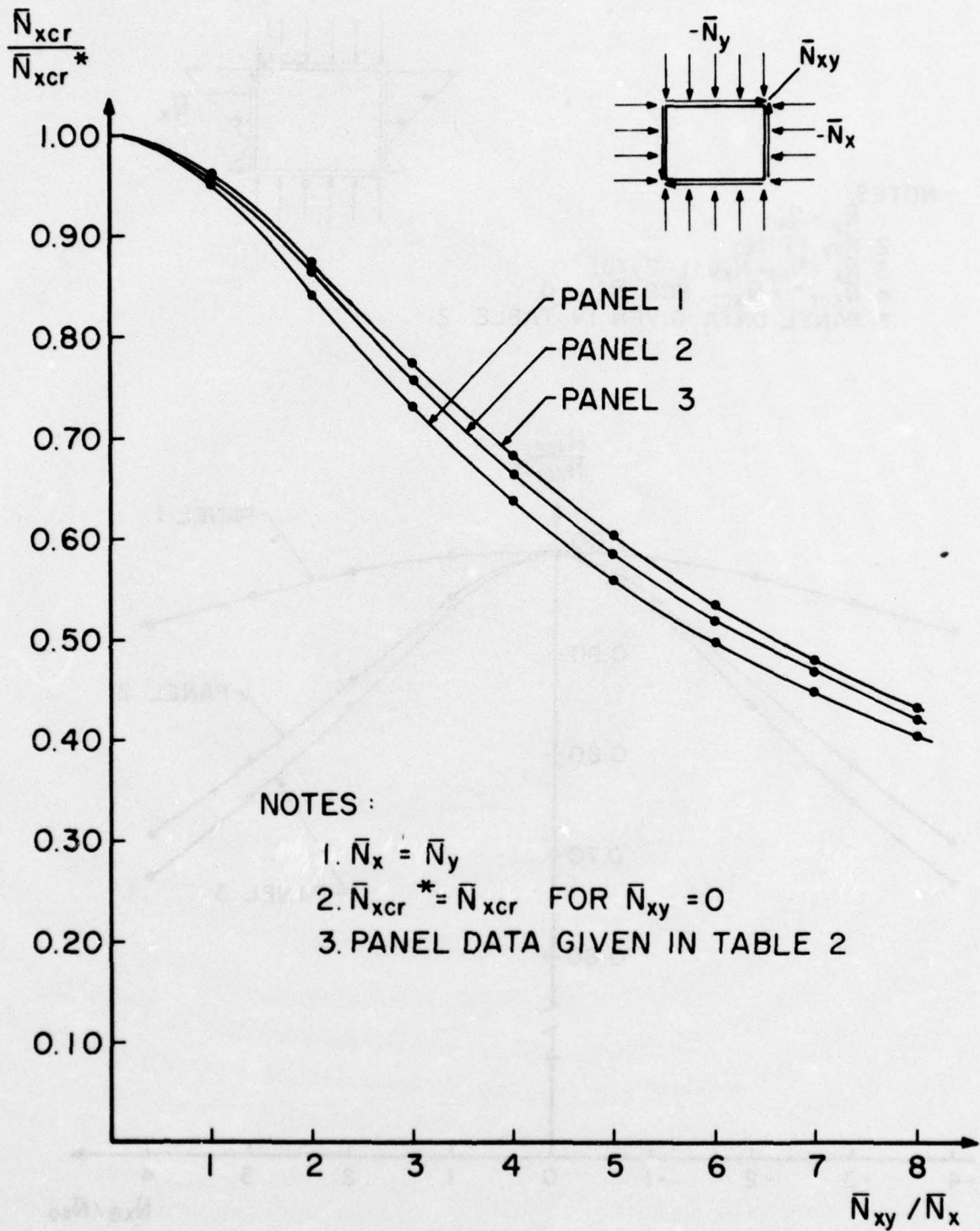
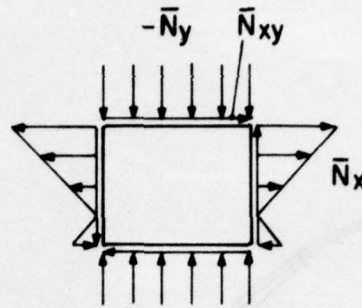


Figure 4. Effect of a Shear Load Upon Critical Compressive Stress in Biaxial Loading.



NOTES:

1. $\bar{N}_y = \bar{N}_{x0}$
2. $\bar{N}_{xy} = 2\bar{N}_{x0}$
3. $\bar{N}_x = \bar{N}_{x0} + \bar{N}_{xB} (1 - 2y/b)$
4. $\bar{N}_{xcr}^* = \bar{N}_{xcr}$ FOR $\bar{N}_{xB} = 0$
5. PANEL DATA GIVEN IN TABLE 2

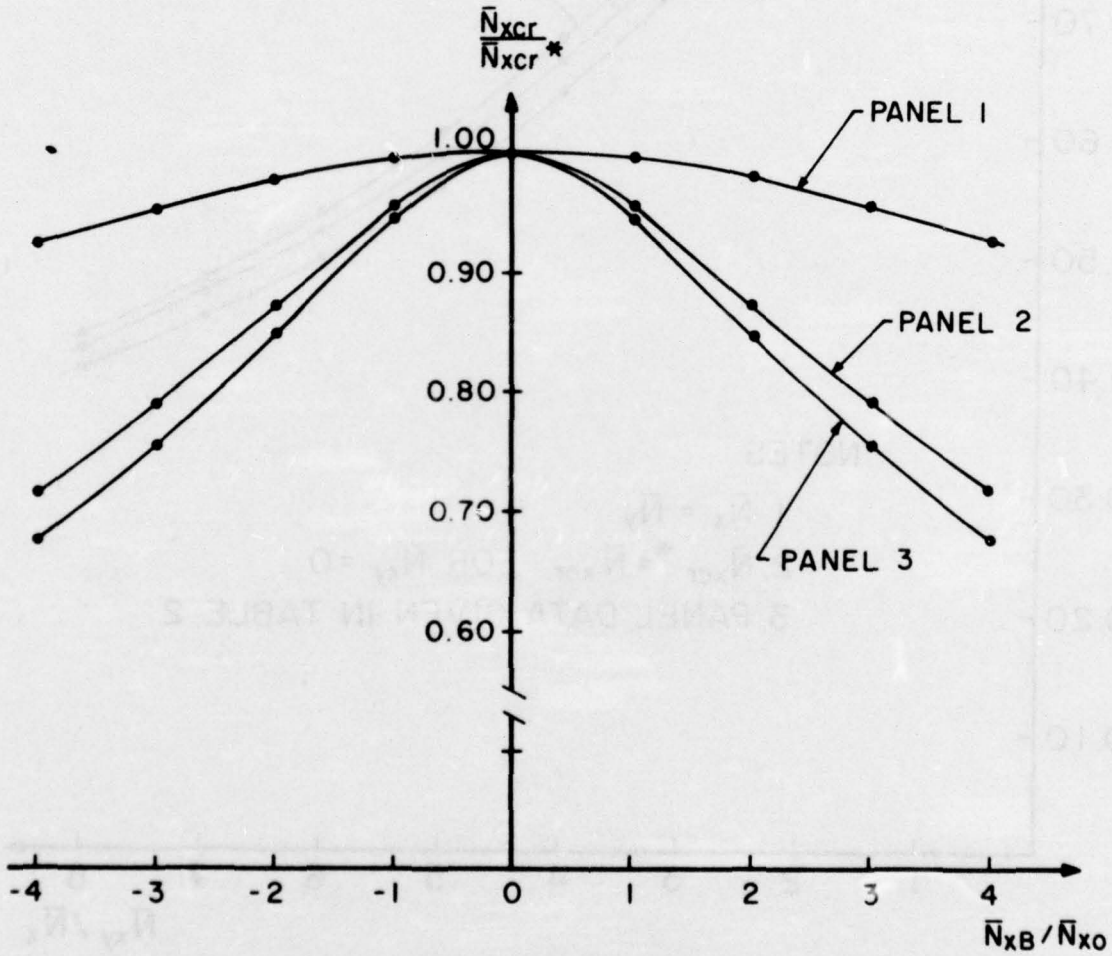


Figure 5. Effect of an Edgewise Bending Load Upon Critical Compressive and Shear Stresses.

TABLE 2: PHYSICAL DATA FOR COMBINED-LOADS EXAMPLES

	Panel 1	Panel 2	Panel 3
E_1	9.5×10^6	10.6×10^6	10.2×10^6
E_2	9.5×10^6	10.6×10^6	10.2×10^6
t_1	.021	.050	.030
t_2	.021	.050	.030
ν_1	.30	.30	.28
ν_2	.30	.30	.28
G_{cxz}	19000.	30000.	8000.
G_{cyz}	19000.	30000.	22000.
t_c	.181	.25	.370
a	20.	20.	32.
b	20.	36.	64.

proportions of edgewise bending stresses are then added to this state of stress, and the resulting loads observed. Results are expressed in terms of the ratio

$$\frac{\bar{N}_{xocr}}{\bar{N}_{xocr}^*} = \frac{\text{Actual critical compressive load}}{\text{Critical compressive load for } \bar{N}_{xB}=0},$$

and the relative magnitude of the bending and direct compressive stresses, $\bar{N}_{xB}/\bar{N}_{xo}$.

4.3 COMPARISON WITH INTERACTION FORMULAS

In order to facilitate the analysis of stability for cases of combined loadings, various interaction formulas have been proposed. A number of examples are given in Reference 1. The purpose of any interaction formula is to account for the combined effects of various applied loads by comparison of the intensity of each load to the critical value of the same load acting alone. Each such ratio is weighted by means of an exponent, associated with the particular type of loading; for example,

$$R_1^{e_1} + R_2^{e_2} = \text{const.},$$

where

$$R_i = \bar{N}_i / \bar{N}_{icr}.$$

The e_i are constant exponents, and the index i is associated with the type of loading.

The use of interaction formulas is attractive since any number of load cases may be analyzed once the individual critical loads are determined. However, such formulas obviously represent approximations to an exact analysis of stability under combined loadings. Interaction formulas for the cases of edgewise compression combined with edgewise shear,

edgewise compression combined with edgewise bending, and edgewise shear combined with edgewise bending have been evaluated to a limited extent during the course of this study.

4.3.1 Interaction Formula for Combined Edgewise Shear and Compression

The interaction formula for axial compression and edgewise shear is¹

$$\bar{N}_x / \bar{N}_{xcr} + (\bar{N}_{xy} / \bar{N}_{xycr})^2 = 1. \quad (4.1)$$

When biaxial compression is present, Equation 4.1 is generalized to the form⁸

$$\bar{N}_x / \bar{N}_{xcr} + \bar{N}_y / \bar{N}_{ycr} + (\bar{N}_{xy} / \bar{N}_{xycr})^2 = 1. \quad (4.2)$$

The left-hand side of Equation 4.2 has been evaluated (see Table 3) for Panels 1 and 2 of Table 2, for various combinations of biaxial compression and shear loads. The formula is reasonably accurate for most of the cases considered. For the square panel (Panel 1) the maximum error observed is .28%. For the rectangular panel (Panel 2) this error increases to more than 11%. It is important to realize that a value of the left-hand side of Equation 4.2 which is greater than one represents a conservative estimate of the critical loads. For all cases included in Table 3, the interaction formula is conservative, with the exception of one example (Case 2-7) involving shear combined with both tension and compression loads.

Equation 4.1 has also been examined for various proportions of compression and shear loads. The error in Equation 4.1 is plotted in Figure 6 as a function of these proportions (a positive error corresponds to a conservative result, as noted previously). Results for the square panel were again very good. Cases tested for the rectangular panel showed a maximum error of approximately 4.5%. Figure 7 shows the compression-shear interaction curves predicted by the present method in relation to a plot of the interaction formula (Equation 4.1).

TABLE 3: COMPARISON WITH INTERACTION FORMULA
FOR COMBINED BIAXIAL COMPRESSION AND
EDGEWISE SHEAR

Case	Panel	n_{x0}	n_{xy}	n_{y0}	\bar{N}_{xcr}	\bar{N}_{xycr}	\bar{N}_{ycr}	Equation 4.2
		1			-421.40			
			1			±881.33		
				1			-421.40	
1-1	1	1	1	1	-200.09	-200.09	-200.09	1.0019
1-2		1	2	1	-177.16	-354.32	-177.16	1.0024
1-3		2	2	1	-257.44	-257.44	-128.72	1.0017
1-4		1	3	2	-118.11	-354.33	-236.22	1.0025
1-5		3	1	0	-411.45	-137.15	0.	1.0006
1-6		1	5	2	-97.66	-488.30	-195.32	1.0022
1-7		2	6	3	-133.98	-401.94	-200.97	1.0028
		1			-1037.24			
			1			±3453.94		
				1			-2331.08	
2-1	2	1	1	1	-759.70	-759.70	-759.70	1.1125
2-2		1	2	1	-683.49	-1366.98	-683.49	1.0942
2-3		2	2	1	-851.82	-851.82	-425.91	1.0648
2-4		2	5	1	-696.10	-1740.25	-348.05	1.0743
2-5		3	7	2	-693.27	-1617.63	-462.18	1.0860
2-6		4	17	1	-553.76	-2353.48	-138.44	1.0576
2-7		-2	4	1	-921.8	1843.6	460.90	.9759

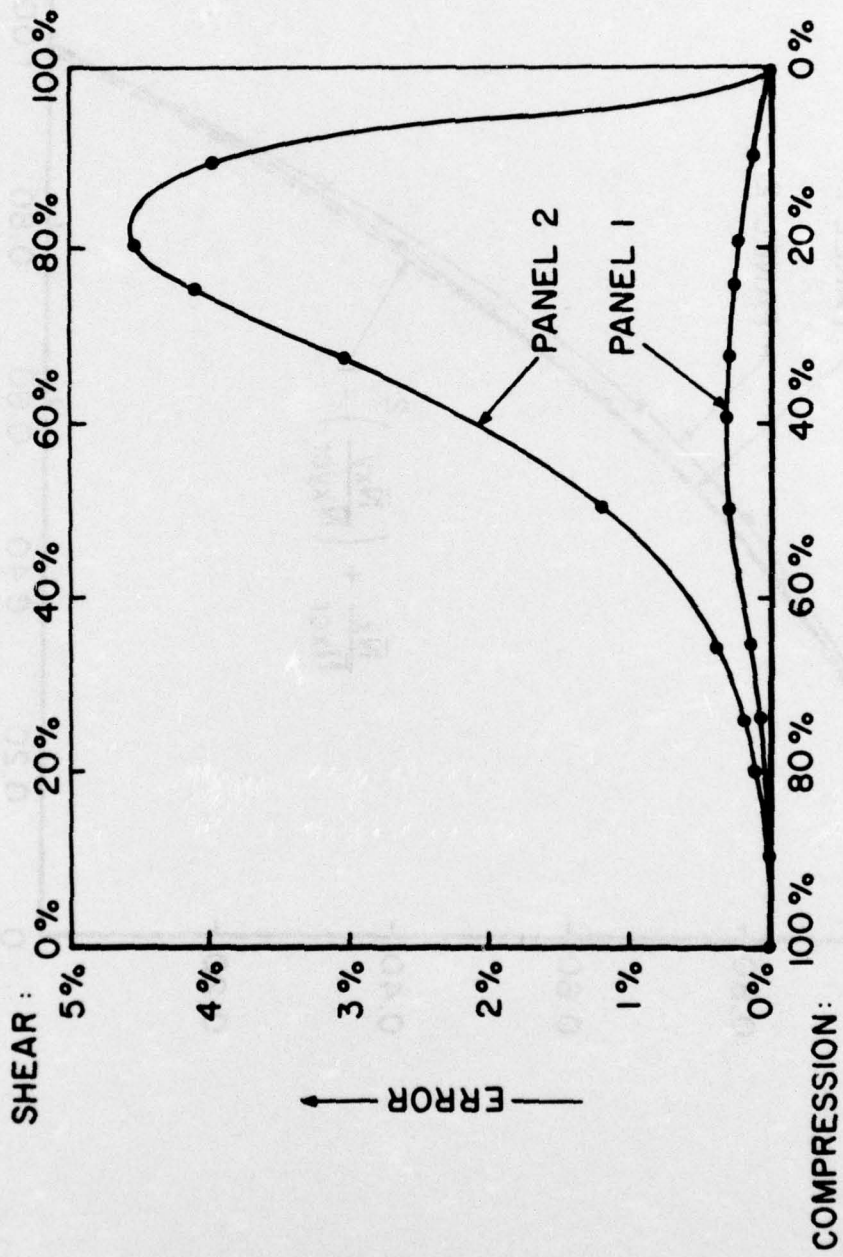


Figure 6. Error in Interaction Formula for Axial Compression and Edgewise Shear.

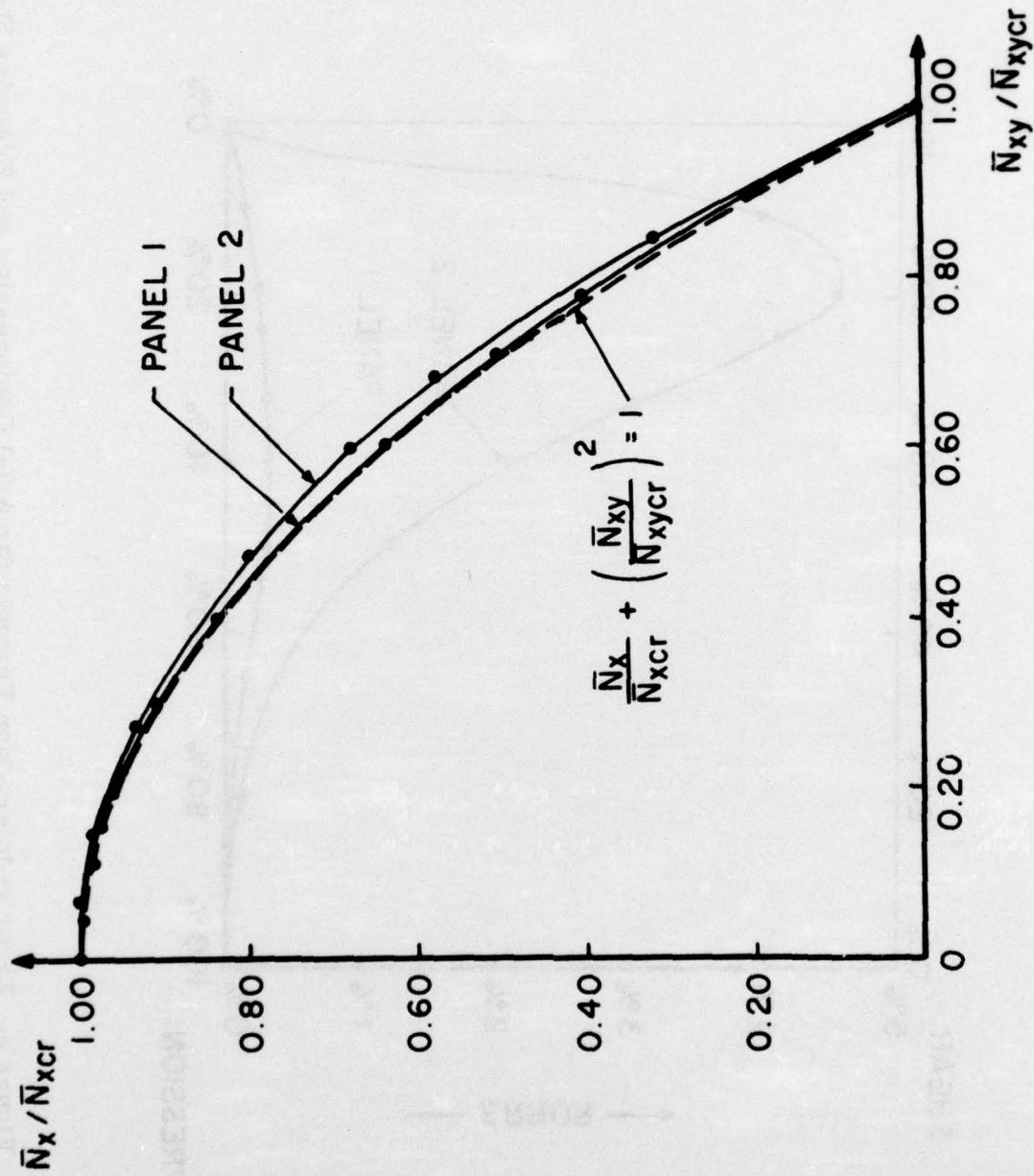


Figure 7. Calculated Interaction Curves for Axial Compression and Edgewise Shear.

4.3.2 Interaction Formula for Combined Edgewise Bending and Compression

The interaction formula for combined edgewise bending and axial compression loads is given by¹

$$\bar{N}_{x_0} / \bar{N}_{x_{ocr}} + (\bar{N}_{x_B} / \bar{N}_{x_{Bcr}})^{3/2} = 1. \quad (4.3)$$

Here \bar{N}_{x_B} is a pure-bending load as shown in Figure 1. Calculated values of the left-hand side of the formula are listed in Table 4, and the corresponding errors are plotted in Figure 8 as a function of the relative proportions of the two loads. Results for the rectangular panel using Equation 4.3 are reasonably good. The maximum error (5.3%) occurs for a moderately large bending load. For the square panel, Equation 4.3 gives accurate results only when the bending load is quite small compared to the compressive force. When the bending load predominates, the error becomes as large as 18%. Again, the interaction formula provides a conservative estimate of the critical load in each case considered. The same results are compared graphically in Figure 9 with the shape of the interaction curve (Equation 4.3).

4.3.3 Interaction Formula for Combined Edgewise Bending and Shear

The interaction formula proposed¹ for the evaluation of critical combined bending and shear loads is

$$(\bar{N}_{x_B} / \bar{N}_{x_{Bcr}})^2 + (\bar{N}_{xy} / \bar{N}_{xy_{cr}})^2 = 1. \quad (4.4)$$

Values of the left-hand side of Equation 4.4, as given in Table 5, indicate nonconservative buckling predictions by the interaction formula. Errors for the square panel considered are less than 8%. Those for the rectangular panel are as high as 13.5%. These values are plotted in Figure 10 for various relative proportions of bending and shear. Critical load combinations are compared to the shape of the interaction curve in Figure 11.

TABLE 4: COMPARISON WITH INTERACTION FORMULA FOR COMBINED EDGEWISE BENDING AND AXIAL COMPRESSION

Case	Panel	n_{xo}	n_{xB}	\bar{N}_{xocr}	\bar{N}_{xBcr}	Equation 4.3
		1		-421.40		
	1		1		± 2387.55	
1-1		1	± 1	-410.67	410.67	1.0459
1-2		2	± 1	-418.60	209.30	1.0193
1-3		3	± 1	-420.14	140.05	1.0112
1-4		6	± 1	-421.08	70.18	1.0043
1-5		1	± 2	-384.17	768.34	1.0942
1-6		1	± 4	-320.17	1280.69	1.1526
1-7		1	± 5	-291.51	1457.56	1.1688
1-8		1	± 6	-266.43	1598.58	1.1801
		1		-1037.24		
	2		1		± 4436.90	
2-1		1	± 1	-972.09	972.09	1.0397
2-2		2	± 1	-1019.04	509.52	1.0214
2-3		3	± 1	-1028.97	342.99	1.0135
2-4		6	± 1	-1035.14	172.52	1.0056
2-5		1	± 2	-847.36	1694.71	1.0530
2-6		1	± 4	-636.13	2544.50	1.0476
2-7		1	± 5	-560.71	2803.54	1.0429
2-8		1	± 6	-500.21	3001.28	1.0386

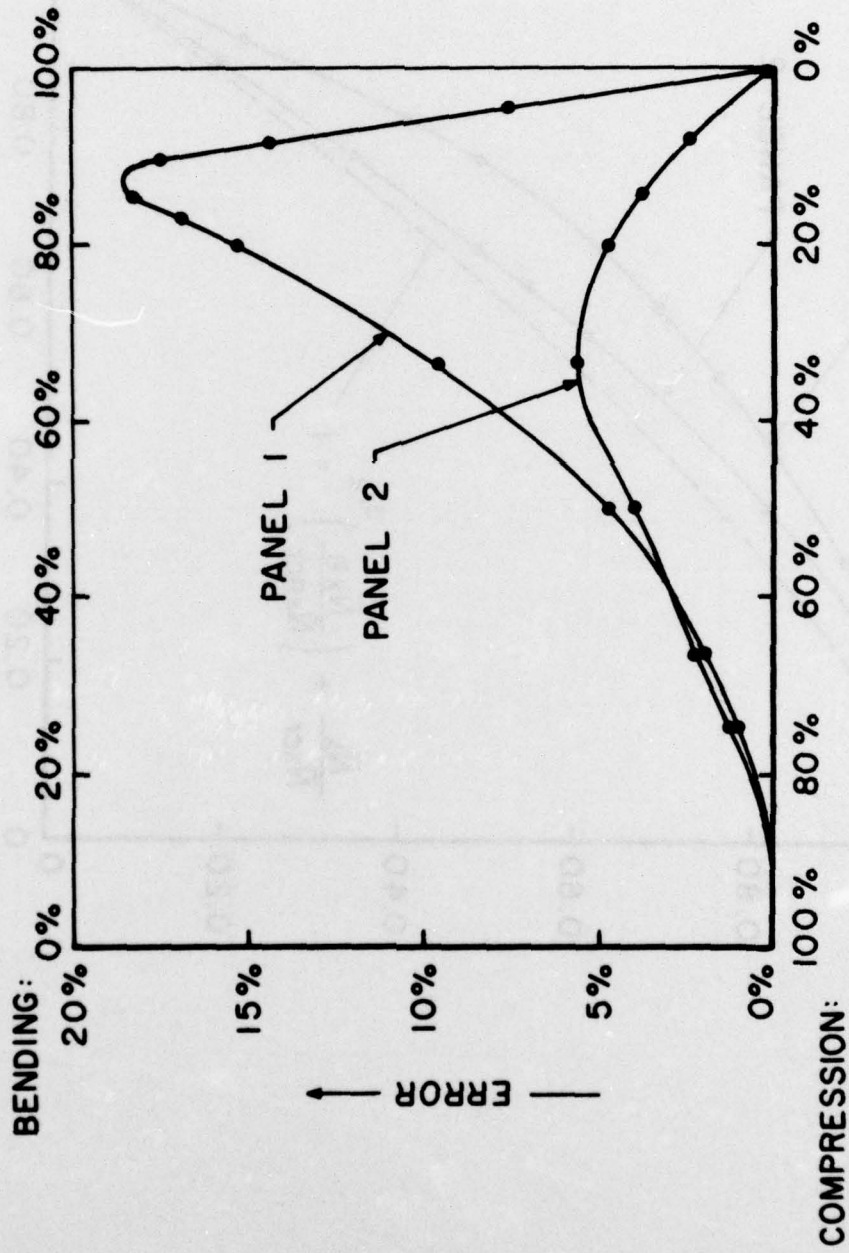


Figure 8. Error in Interaction Formula for Edgewise Bending and Compression.

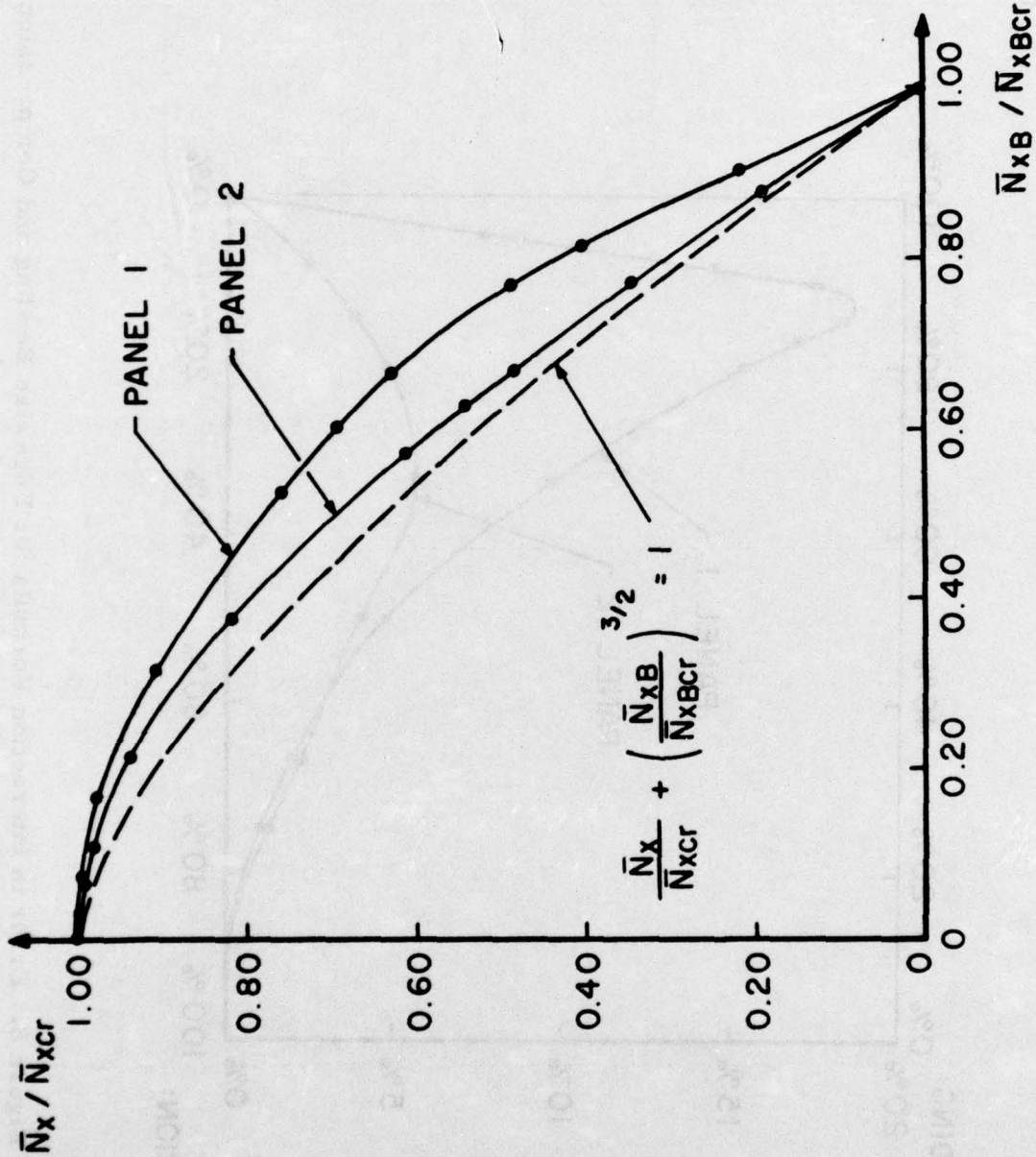


Figure 9. Calculated Interaction Curves for Edgewise Bending and Compression.

TABLE 5: COMPARISON WITH INTERACTION FORMULA FOR
COMBINED EDGEWISE BENDING AND SHEAR

Case	Panel	n_{xB}	n_{xy}	\bar{N}_{xB}	\bar{N}_{xy}	Equation 4.4
		1		± 2387.55		
			1		± 883.78	
1-1	1	1	1	815.29	815.29	.9676
1-2		-1	1	815.29	815.29	.9676
1-3		2	1	1370.34	685.17	.9305
1-4		4	1	1900.11	475.03	.9223
1-5		1	3	291.69	875.07	.9953
1-6		1	5	176.12	880.61	.9983
1-7		1	8	110.32	882.53	.9993
1-8		1	10	88.30	882.98	.9996
		1		± 4436.90		
			1		± 3453.94	
2-1	2	1	1	2534.14	2534.14	.8645
2-2		-1	1	-2534.14	2534.14	.8645
2-3		2	1	3534.07	1767.04	.8962
2-4		4	1	4131.24	1032.81	.9564
2-5		1	3	1074.01	3222.02	.9288
2-6		1	5	668.70	3343.49	.9598
2-7		1	8	425.15	3401.19	.9789
2-8		1	10	341.79	3417.89	.9852

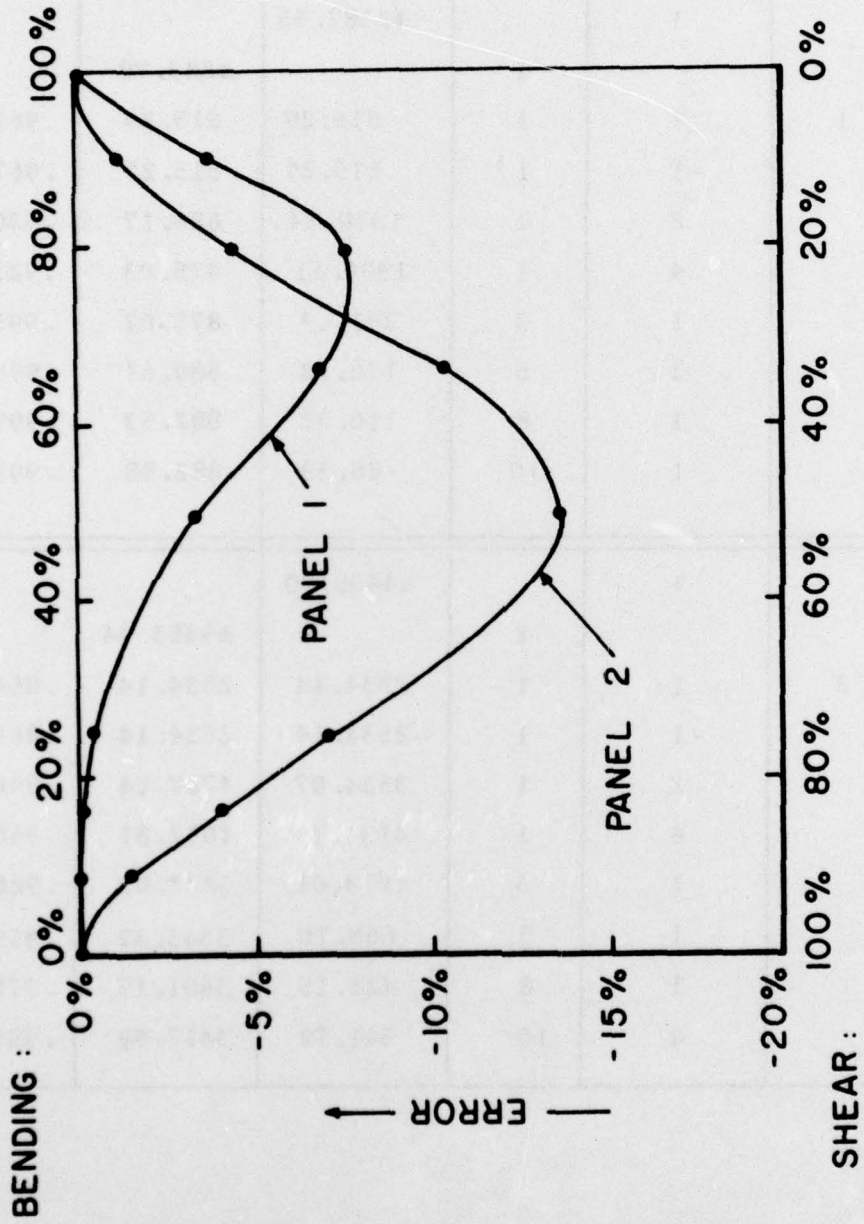


Figure 10. Error in Interaction Formula for Edgewise Shear and Bending.

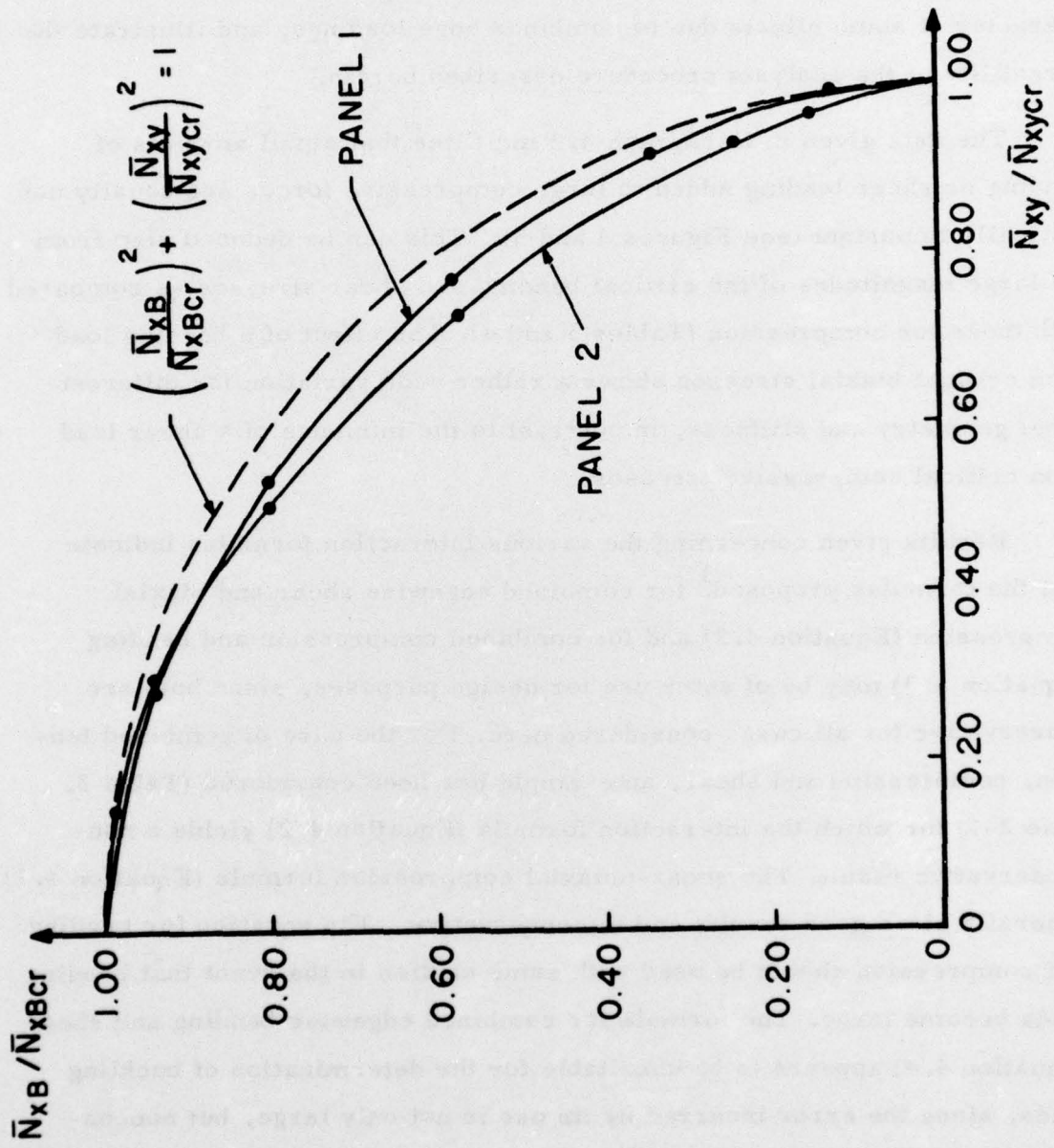


Figure 11. Calculated Interaction Curves for Combined Edgewise Shear and Bending.

4.4 DISCUSSION

Various calculations concerning the stability of a sandwich panel under combined modes of loading and the effectiveness of typical interaction formulas have been presented in this section. These results indicate the character of some effects due to combined edge loadings, and illustrate the versatility of the analysis procedure described herein.

The data given in Paragraph 4.2 indicates that small amounts of bending or shear loading added to large compressive forces are usually not critically important (see Figures 4 and 5). This can be deduced also from the large magnitudes of the critical bending and shear stresses as compared with those for compression (Tables 3 and 4). The effect of a bending load upon critical biaxial stresses shows a rather wide variation for different panel geometry and stiffness, in contrast to the influence of a shear load upon critical compressive stresses.

Results given concerning the various interaction formulas indicate that the formulas proposed¹ for combined edgewise shear and biaxial compression (Equation 4.2) and for combined compression and bending (Equation 4.3) may be of some use for design purposes, since both are conservative for all cases considered here. For the case of combined tension, compression and shear, an example has been considered (Table 3, Case 2-7) for which the interaction formula (Equation 4.2) yields a non-conservative result. The shear-uniaxial compression formula (Equation 4.1) generally gives good results and is conservative. The equation for bending and compression should be used with some caution in the event that bending loads become large. The formula for combined edgewise bending and shear (Equation 4.4) appears to be unsuitable for the determination of buckling loads, since the error incurred by its use is not only large, but nonconservative.

SECTION 5

SUMMARY AND CONCLUSIONS

An analysis procedure has been described for the prediction of the general instability of flat, simply-supported, rectangular sandwich panels loaded by arbitrary combinations of biaxial edgewise compression, biaxial edgewise bending, and edgewise shear forces. The mathematical model is formulated in terms of the total potential energy, which is composed of the internal elastic strain energy of the sandwich plate and the potentials of the applied loadings. The Ritz method is used to transform the energy functional in terms of continuous field variables into a quadratic function of certain discrete parameters. Application of the principle of minimum potential energy results in a generalized discrete eigenvalue problem, which can be solved by standard methods. The finite number of eigenvalues obtained in the solution approximate the lowest of the infinite number of critical loads, while the eigenvectors approximate the corresponding buckled mode shapes.

The accuracy of the analysis has been demonstrated by comparison with results available in the literature for a number of examples. A limited study has been made of the applicability of typical interaction formulas which are commonly used in sandwich design. Comparisons of the interaction formulas with numerical results generated from the present analysis indicates that certain of these formulas can yield substantially nonconservative results for some combinations of geometry and loading, and should be used with caution.

A computer program has been developed for the implementation of the combined-loads instability analysis. The program is operable both interactively and by batch mode processing. A detailed description of the computer program and its usage are contained in a companion report.¹⁷

The analysis presented has been demonstrated to be a useful tool for the stability analysis of a practical class of sandwich panels. However, a number of extensions could be undertaken to apply the analysis to more general situations. Remaining within the confines of the linear formulation, extensions of the present method to include layered composite faces, elastic edge members, and more general panel shapes should be given consideration. The analysis can be generalized to the cases of multicore sandwich and panels having normal deformations, at some expense in the number of degrees of freedom to be considered. The consideration of boundary conditions other than simple supports are accommodated by altering the assumed-mode functions to be used in the Ritz approximations. However, the computational effort is increased for more general support conditions, since the normal displacement does not uncouple from the other displacement variables, as is the case for simply-supported boundaries (see Equations 3.6 and 3.7).

In conclusion, the sandwich instability analysis described in this report represents a useful and accurate tool for the design and analysis of lightweight, high-performance structural components. In addition, the method reported provides a suitable starting point for the consideration of many more general types of sandwich construction.

SECTION 6
REFERENCES

1. MIL-HDBK-23A, "Structural Sandwich Composites," U.S. Department of Defense, Washington, D. C., December 1968.
2. Kuenzi, E. W., "Buckling Coefficients for Simply Supported, Flat, Rectangular Sandwich Panels under Biaxial Compression," Forest Products Laboratory Report 1558, 1946.
3. Norris, C. B., "Compressive Buckling Curves for Flat Sandwich Panels with Dissimilar Facings," Forest Products Laboratory Report 1875, 1960.
4. March, H. W., "Effects of Shear Deformation in the Core of a Flat Rectangular Sandwich Panel," Forest Products Laboratory Report 1583, 1948.
5. March, H. W., and C. B. Smith, "Buckling Loads of Flat Sandwich Panels in Compression -- Various Types of Edge Conditions," Forest Products Laboratory Report 1525, 1945.
6. Hoff, N. J., "Bending and Buckling of Rectangular Sandwich Plates," NACA TN2225, 1950.
7. Kuenzi, E. W., W. S. Ericksen, and J. J. Zahn, "Shear Stability of Flat Panels of Sandwich Construction," Forest Products Laboratory Report 1560, Revised 1962.
8. Norris, C. B., and W. J. Kommers, "Critical Loads of a Rectangular, Flat Sandwich Panel Subjected to Two Direct Loads Combined with a Shear Load," Forest Products Laboratory Report 1833, 1952.
9. Sullins, R. T., G. W. Smith, and E. E. Spier, "Manual for Structural Stability Analysis of Sandwich Plates and Shells," NASA CR-1457, General Dynamics Corp., San Diego, California, December 1969.
10. Kimel, W. R., "Elastic Buckling of a Simply Supported Rectangular Sandwich Panel Subjected to Combined Edgewise Bending and Compression," Forest Products Laboratory Report 1857, 1956.

11. Kimel, W. R., "Elastic Buckling of a Simply Supported Rectangular Sandwich Panel Subjected to Combined Edgewise Bending, Compression and Shear," Forest Products Laboratory Report 1859, 1956.
12. Bogner, F. K., "Theory of Sandwich Plates," University of Dayton Research Institute, UDRI-TR-76-01.
13. Habip, L. M., "A Survey of Modern Developments in the Analysis of Sandwich Structures," Applied Mechanics Review, Vol. 18, No. 2, 1965.
14. Washizu, K., Variational Methods in Elasticity and Plasticity, Pergamon Press, New York, 1968.
15. Monforton, G. R., "Discrete Element, Finite Displacement Analysis of Anisotropic Sandwich Shells," Rept. No. 39, Division of Solid Mechanics, Structures and Mechanical Design, School of Engineering, Case Western Reserve University, January 1970.
16. Timoshenko, S. P. and J. M. Gere, Theory of Elastic Stability, 2nd Edition, McGraw Hill Book Co., New York, 1961.
17. Brockman, R. A., "Computer Program for the Stability Analysis of Flat, Simply Supported, Rectangular Sandwich Panels Subjected to Combined Inplane Loadings," University of Dayton Research Institute, UDRI-TR-76-02.